Synthesis of Imidazolium Compounds as Model Substrates for Biomimetic Mono-Iron Hydrogenase Complexes

Eileen Sullivan

In partial fulfillment of the requirements for graduation with the Dean's Scholars Honors Degree in Biochemistry

_____ _____

Michael J. Rose Date
Supervising Professor

_____ _____

Jeffrey E. Barrick Date
Honors Advisor in Biochemistry

I grant the Dean's Scholars Program permission to post a copy of my thesis on the Texas ScholarWorks. For more information, visit https://repositories.lib.utexas.edu/.

Synthesis of Imidazolium Compounds as Model Substrates for Biomimetic Mono-Iron Hydrogenase Complexes

Department: Chemistry and Biochemistry

_____
Student

_____ _____
Signature Date

_____
Supervising Professor

_____ _____
Signature Date

Abstract

As the demand for carbon-free fuel sources has increased, hydrogen gas has become a promising alternative since it can be produced from water. However, efficient production of H_2 requires the use of expensive metal catalysts such as platinum. Because of the cost and low availability of these metals, scientists have turned to nature as inspiration for the development of metal catalysts that use cheaper, more abundant transition metals. One such example of a natural H_2 catalyst is the mono-iron hydrogenase enzyme, which heterolytically cleaves H_2 into a proton and hydride. The active site of this enzyme contains a central iron atom surrounded by a nitrogen-bound pyridone, an acyl carbon, and a cysteine thiolate donor. This unique arrangement of ligands allows the enzyme to activate H_2 with the help of the substrate, methenyl-H_4MPT^+. Previous research by the Rose Group has led to the development of a functional biomimetic model of the mono-Fe hydrogenase active site that is capable of activating H_2. This biomimetic model can accept a hydride from the substrate, but the reverse reaction of hydride transfer to the substrate had yet to be observed. To achieve this, obtaining more information about the role of the substrate in H_2 activation was necessary. This research therefore focused on the synthesis of a model imidazolium substrate based on methenyl- H_4MPT^+. In reactivity studies with an enzyme model, it was determined that altering the Lewis acidity of the model substrate promoted hydride transfer from the model complex. With this insight, it is hoped that the interaction between the endogenous substrate and the mono-iron hydrogenase active site can be better understood.

Table of Contents

Introduction……..…..**1**

Results and Discussion…….....…..**9**

I. Synthesis of Imidazolium Derivatives……...……**10**

II. Imidazolium Reactivity based on Lewis Acidity……..…….….**14**

III. Imidazolium as both a Ligand and Substrate…….…….**20**

Conclusion…….…….…..….**23**

Materials & Methods….…….…….……..……..**23**

References…….....…**31**

Supporting Information…….…….....……**33**

Introduction

The world currently relies heavily on hydrocarbon sources such as coal or natural gas for energy production. In 2011, over 80% of total primary energy came from fossil fuels. [1] While efficient, these sources of energy produce carbon dioxide and other pollutants that damage the environment, and they are limited in supply. [1] Hydrogen has recently proven to be a viable and cleaner alternative form of energy. Unlike fossil fuels, hydrogen can be produced from the electrolysis of water using solar energy. By passing an electric current through water, the H_2O molecules can be split into oxygen and hydrogen gas.[2] If the electricity needed to power electrolysis was generated by solar, wind, or nuclear sources, zero greenhouse gasses would be produced. Because of this, hydrogen is a promising renewable fuel source.

However, hydrogen production by electrolysis is not yet efficient for large-scale use. The amount of energy required to electrolytically split water into oxygen and hydrogen is ultimately more than the energy available from the hydrogen produced.[3] Additionally, producing hydrogen by electrolysis is more expensive than the more common steam reforming method.[4] One reason for this high cost is the need for not only electricity, but also expensive metal catalysts such as platinum or palladium. Compared to other transition metals, platinum and palladium are more expensive and less earth-abundant, posing an economic barrier to electrolysis. Therefore, production of H_2 as an energy source needs to overcome many hurdles before it will be feasible for large-scale energy use.

One way researchers are trying to solve these issues is through the exploration of new hydrogen catalysts. Instead of developing these catalysts from scratch, scientists have turned to biology for inspiration. Many microorganisms are able to utilize H_2 as an energy source due to the presence of several hydrogenase enzymes. In bacteria, this enzyme supplies energy for anaerobic

metabolism and can act as an electron acceptor, resulting in the production of H_2.[5] In general, the hydrogenase enzymes function by activating the H_2 bond through interaction with metal(s) in the enzyme's active site. There are currently three phylogenetically distinct forms of hydrogenase that are known, each with a unique active site: [Fe-Fe] hydrogenase, [Ni-Fe] hydrogenase, and mono-[Fe] hydrogenase (Figure 1).

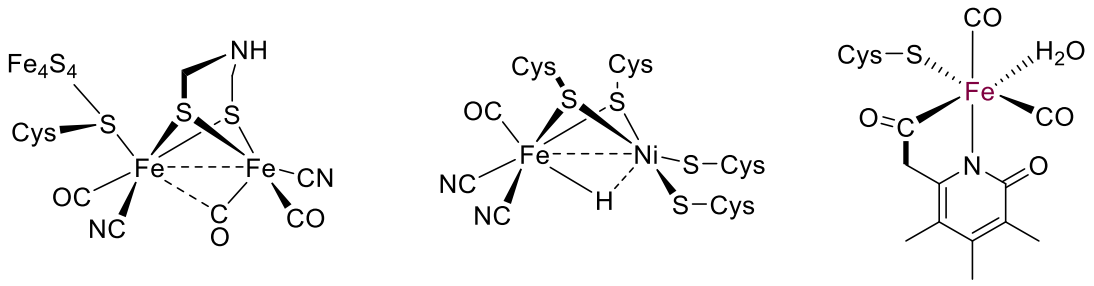

Figure 1. Active sites of [Fe-Fe] hydrogenase (left), [Ni-Fe] hydrogenase (center), and mono-[Fe] hydrogenase (right)

[Fe-Fe] hydrogenases catalyze the reaction of H_2 into protons and electrons ($H_2 \leftrightarrow 2H^+ + 2e^-$). They are most commonly found in anaerobic prokaryotes or unicellular algae as a way to prevent buildup of excess electrons or reducing equivalents.[6] As its name suggests, the active site of di-iron hydrogenase is composed of two iron atoms, connected by two bridging thiolates and a bridging carbonyl. The coordinated CN^- ligands are thought to help stabilize the Fe-Fe orientation in the protein during catalysis. The CO ligands however are more labile and can take on different configurations during the catalytic cycle.[7] Due to their high catalytic activity, [Fe-Fe] hydrogenases have been extensively studied for hydrogen production. Comparatively, the [Ni-Fe] hydrogenase catalyzes the same reversible reaction as [Fe-Fe] hydrogenase, producing protons and electrons from H_2. Like [Fe-Fe] hydrogenase, this class of hydrogenase also contains an iron-sulfur cluster, which is thought to play a role in electron transport. In both enzymes, the active sites are coordinated by cysteine residues from the surrounding protein and contain CN^- and CO ligands. However, this enzyme differs in that it contains a Ni atom in place of one of the Fe atoms in the

active site. Additionally, the active site consists of two bridging thiolates, and an open coordination site between the Ni and Fe metals. Unlike [Fe-Fe] hydrogenase, [Ni-Fe] hydrogenase appears to prefer H_2 oxidation over the reverse reaction.[6] However, it has also been frequently studied due to its abundance in many types of bacteria, including anaerobic and pathogenic organisms.[11]

As the third type of hydrogenase to be discovered, mono-[Fe] hydrogenase is presently the least studied. Only relatively recently, in 2009, was a complete crystal structure of the enzyme's active site solved.[9] However, valuable information has been learned since then. Mono-[Fe] hydrogenase differs from the other hydrogenases in both structure and function. Instead of catalyzing the redox reactions of H_2, this enzyme heterolytically cleaves H_2 into a proton and hydride ($H_2 \leftrightarrow H^+ + H^-$). The active site of the mono-[Fe] hydrogenase is unique in that in contains a single iron center that is not redox-active. Additionally, it has a unique arrangement of covalently bound compounds, called ligands, that assist in hydrogen activation. Unlike the [Fe-Fe] and [Ni-Fe] active sites, this enzyme does not contain an iron-sulfur cluster or CN^- ligands. Instead, mono-[Fe] hydrogenase relies on coordination by a nitrogen-bound pyridone, an acyl carbon, and a sulfur thiolate donor. From previous enzyme models, it is believed that all three of these ligands are important for hydrogen activation (Figure 2).[8,9]

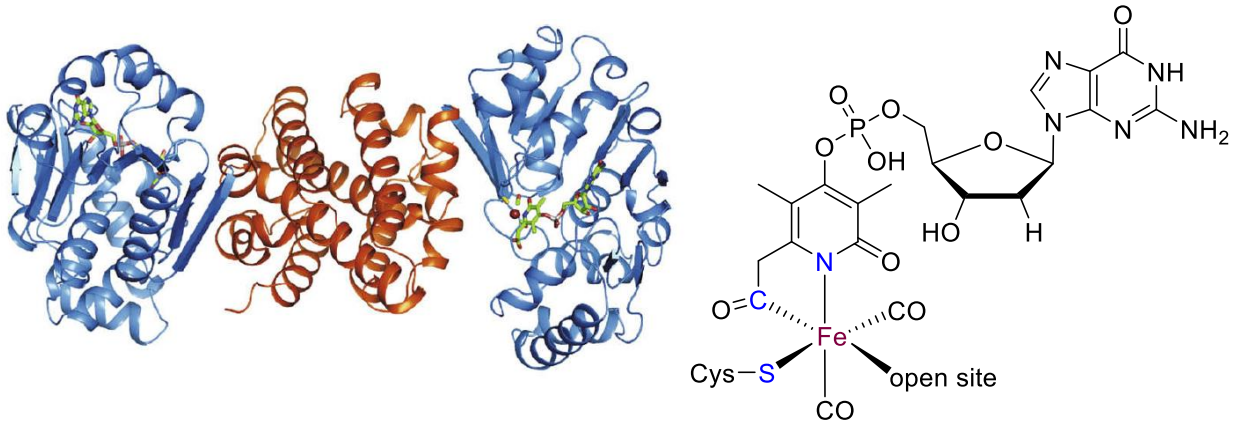

Figure 2. Active site of mono-[Fe] hydrogenase with facial arrangement of N, C, and S atoms, Cys_{176}, and an open site *trans* to the acyl unit.[9]

As the least-studied and most unique class of hydrogenase, it is important to learn more about the function of mono-[Fe] hydrogenase. One way this is possible is through the design of small molecule mimics of the enzyme active site that display similar catalytic activity to the natural enzyme. Typically, enzymes are studied by manipulating single amino acid residues in the active site and observing the resulting effects on structural, kinetic, and binding parameters. However, the active site of mono-[Fe] hydrogenase contains only a single cysteine residue bound to the Fe center, making it less suitable for this type of study. By preparing small molecule mimics of mono-[Fe] hydrogenase through synthetic organic and inorganic chemistry, the various features of the active site (pyridone, thiolate, substrate) can be more easily modulated and studied. Synthetic models of [Fe-Fe] and [Ni-Fe] hydrogenases would be useful, but their mechanisms have already been more extensively studied. Additionally, they have been shown to be more susceptible to oxygen exposure, making reactivity studies difficult.[6] The presence of only a single metal center in the mono-[Fe] active site makes it not only simpler to model, but important to study for comparison to the other hydrogenases. Therefore, one goal of this project is to help characterize and evaluate a small model mimic of mono-[Fe] hydrogenase.

Looking more closely at the natural enzyme, the role of the substrate is also important for hydrogen activation. Mono-[Fe] hydrogenase is commonly found in methanogenic archaea that utilize H_2 to reduce CO_2 to methane. Within this process, the enzyme interacts selectively with a substrate called methenyltetrahydromethanopterin (methenyl-H_4MPT+), and transfers a hydride to it, forming methyleneltetrahydromethanopterin (methylene-H_4MPT).[10] In nature, the reverse reaction can also occur in which methylene-H_4MPT transfers the hydride back to the Fe center of the active site (Figure 3). From there it can combine with H^+ and release H_2. An effective synthetic model of the enzyme should therefore be able to catalyze $H_2 \leftrightarrow H^+ + H^-$ in both directions with the assistance of a model substrate.

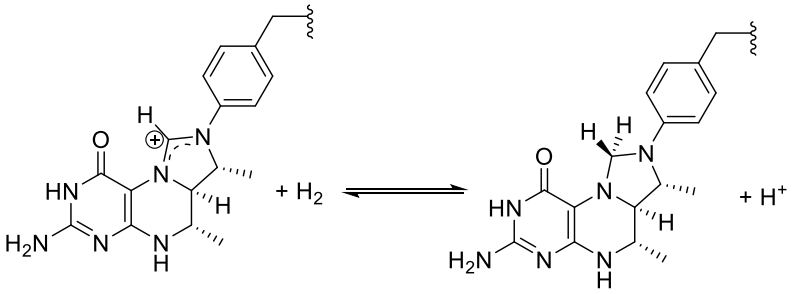

Figure 3. Role of mono-[Fe] hydrogenase in the reversible reduction of the substrate methenyl-H_4MPT^+ to methylene-H_4MPT.

In the Rose Group, a current model of mono-[Fe] hydrogenase has shown to be capable of catalyzing the reverse reaction in which H_2 is produced. This model differs from previous models in that it obtains the correct facial chelation of the nitrogen, carbon, and sulfur atoms present in the natural enzyme (Figure 4).[9] This means that the N, C, and S atoms are all in the same face of the central Fe atom. The positioning of an open coordination site *trans* to the carbamoyl group also closely models the natural enzyme. However, it differs from the natural enzyme in that it incorporates a pyridine moiety instead of a pyridone, a thioether in place of the natural thiolate, and a carbamoyl group (RN-C=O) in place of an acyl group.[8] This model is referred to as the Fe-carbamoyl model due to the presence of the Fe-$C_{carbamoyl}$ bond.

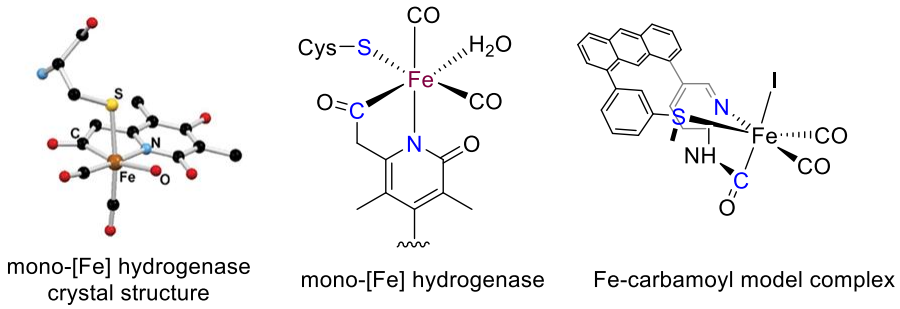

Figure 4. Solved crystal structure of mono-[Fe] hydrogenase (left) [9], and comparison of natural enzyme active site (middle) with biomimetic Fe-carbamoyl model (right)

Despite these differences, this model has shown promising results. Reactivity studies performed with this model showed that in the presence of a base (phenolate), model substrate (imidazolidine), and H_2 gas, the Fe center was competent for hydride abstraction and producing H_2 ($H^+ + [C\text{-}H] \rightarrow H_2 + [C+]$). The proposed mechanism for this model complex is shown in Figure 5.

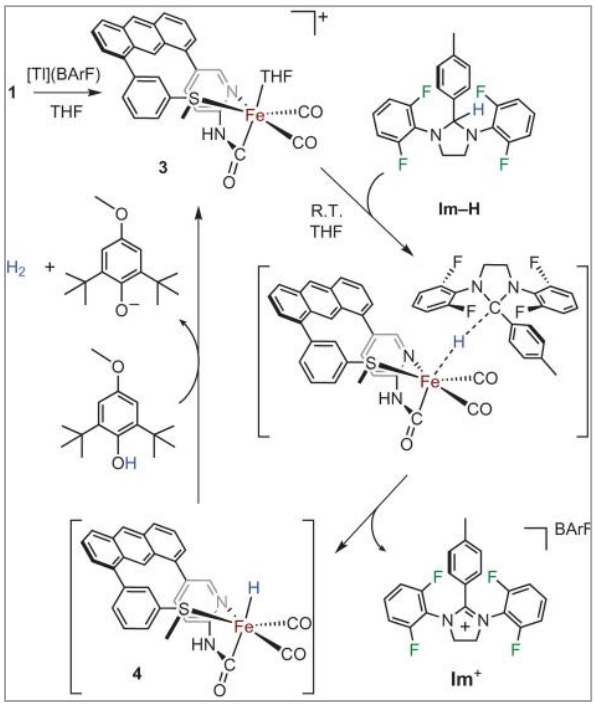

Figure 5. Proposed mechanism for the reactivity of the Fe-carbamoyl model with H_2 in the presence of an imidazolidine substrate and 2,6-di-*tert*-butyl-4-methoxyphenol. [8]

In this mechanism, an iodide atom attached to the open site of the iron center (not shown) is first replaced by THF. Addition of the model substrate, imidazolidine (Im-H), is thought to

produce an intermediate in which the iron center interacts with the nascent hydride from the imidazolidine. The hydride eventually transfers completely to the Fe center as evidenced by the formation of imidazolium (Im^+). Observation of a deprotonated base and H_2 gas suggest that the reaction is catalytic.[8]

One important feature of this mechanism is the role of the imidazolidine substrate (1,3-bis(2,6-difluorophenyl)-2-(4-tolyl)imidazolidine). For discussion purposes, it will be abbreviated Im-H and the dehydrided form (imidazolium) will be abbreviated Im+. In the natural enzyme, the substrate involved is methylene-H_4MPT. Both the model and natural substrate have the same imidazolidine structure (two nitrogen atoms separated by one carbon in a five-member ring). Following hydride abstraction, both will form a carbocation in the same position. Their role as Lewis acids make them capable of accepting an electron pair, such as from a hydride. This acidity also allows them to interact well with a metal center. Since this is the main site for hydrogen activation, it appears that the model imidazolidine is an effective mimic of the natural substrate (Figure 6).

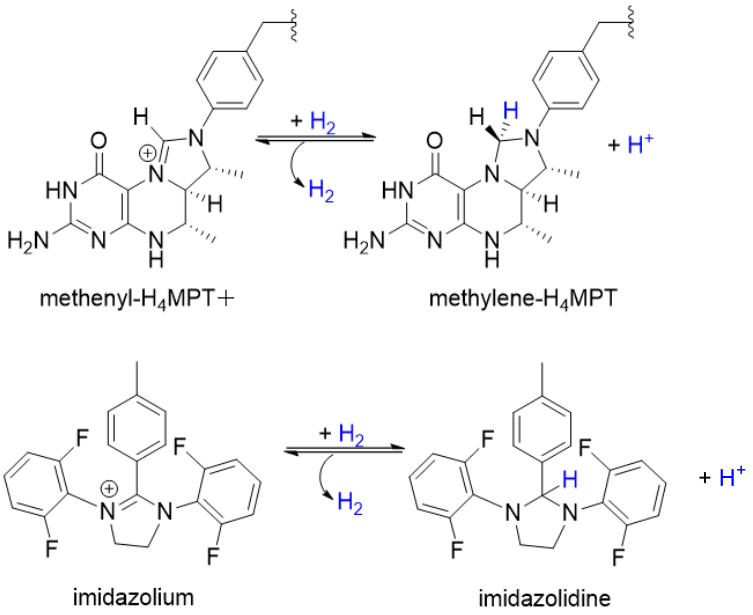

Figure 6. Comparison of H_2 reactivity with the natural mono-[Fe] hydrogenase substrate (top) and with the model imidazolium substrate (bottom)

However, using the Fe-carbamoyl model complex, the reverse reaction in which a hydride is abstracted from the Fe center by the imidazolium substrate (Im+) has not yet been observed. This reaction is necessary to further prove that the enzyme model is catalytic, and functions in both the forward and reverse directions like the natural enzyme. The lack of success in observing hydrogenation of the imidazolium substrate may be attributed to several important factors. One reason may be that the imidazolium (Im+) used in the study was not a strong enough hydride acceptor, making it unable to abstract the hydride from the Fe center. It is proposed that increasing the Lewis acidity or altering the electronics of the model imidazolium substrate by attaching various electron-donating/withdrawing groups to the *para* position on the imidazolium will assist in observing hydride transfer to the substrate. Therefore, one goal of this research will be to modulate the electronics of this substrate to determine its role in hydrogen activation by the enzyme in both the forward and reverse directions. This paper will discuss the synthesis and

resulting reactivity studies of various imidazolium substrates involved in the reactivity of a model mono-[Fe] hydrogenase.

A second reason the reverse hydrogenation reaction may not have been observed could be that the model is not as effective as the natural enzyme at adjusting its Lewis acidity/basicity, and is presently better suited for hydride abstraction.[8] One reason for this modulation difficulty may be due to the absence of a pyridone in the model. As stated earlier, the existing model has a pyridine in place of the pyridone of the native enzyme. While this does not seem like a large difference, the C=O oxygen present in a pyridone is capable of interacting with hydrogen atoms, potentially stabilizing them in the active site until the desired reaction has occurred. Through the synthesis of pyridone analogs it is hoped that a chemical model closer in structure to the actual mono-[Fe] hydrogenase can be synthesized. Substitution of the various pyridone analogs into a working model of the enzyme is a long-term goal of this project (not discussed further herein).

The scope of this research covers the synthesis of various imidazolium compounds to determine the importance of the substrate in H_2 activation. Reactivity studies with the synthesized imidazoliums will probe whether hydride transfer from H_2 to the substrate is possible with the enzyme model.

Results and Discussion

Imidazoliums are derived from the imidazole functional group, which is a heterocyclic five-membered aromatic ring containing two nitrogen atoms. An imidazolium is the cationic species formed by the addition of hydrogen to an imidazole. It can easily be converted to an imidazolidine through addition of a hydride. These compounds are important to many chemical and biological fields due to their Lewis acidity.[12] The positive charge, which exists as a resonance structure between the two nitrogen atoms, allows the imidazolium to accept an electron pair, such

as a hydride or a Lewis base. Meyer et al. first described the synthesis of an imidazolium that would be a suitable substrate for mono-[Fe] hydrogenase due to its similarity to methenyl-H_4MPT^+.[13] Their synthetic approach has been expanded to synthesize six different imidazolium derivatives (Figure 7).

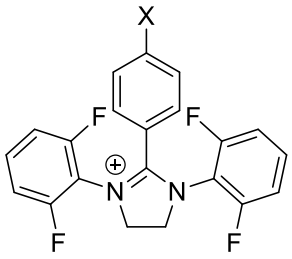

X = CF_3, Br, H, CH_3, OMe

Figure 7. Imidazolium derivatives synthesized based off Meyer et al. procedure. The derivatives vary in electron donating/withdrawing abilities, causing the overall compounds to have varying Lewis acidities

I. Synthesis of Imidazolium Derivatives

The synthesis of each imidazolium was achieved through a three-step synthetic route based on the procedure of Meyer et al. The first step involved preparation of trimethylsilyl polyphosphate (PPSE), a known dehydrating reagent in the synthesis of amines and symmetric amidines (Scheme 1).[14]

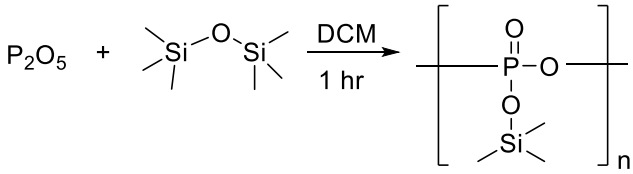

Scheme 1. Preparation of PPSE with phosphorous pentoxide and hexamethyldisiloxane

This reaction activates hexamethyldisiloxane with phosphorous pentoxide in the presence of dichloromethane (DCM) to produce a mixture of cyclic and linear tetraphosphoric acid esters (Figure 8). These products comprise the active species in PPSE. Compared to the more commonly known reagent polyphosphoric acid (PPA), PPSE is beneficial in the synthesis of amines and amidines in that it is aprotic and soluble in organic solvents.[15]

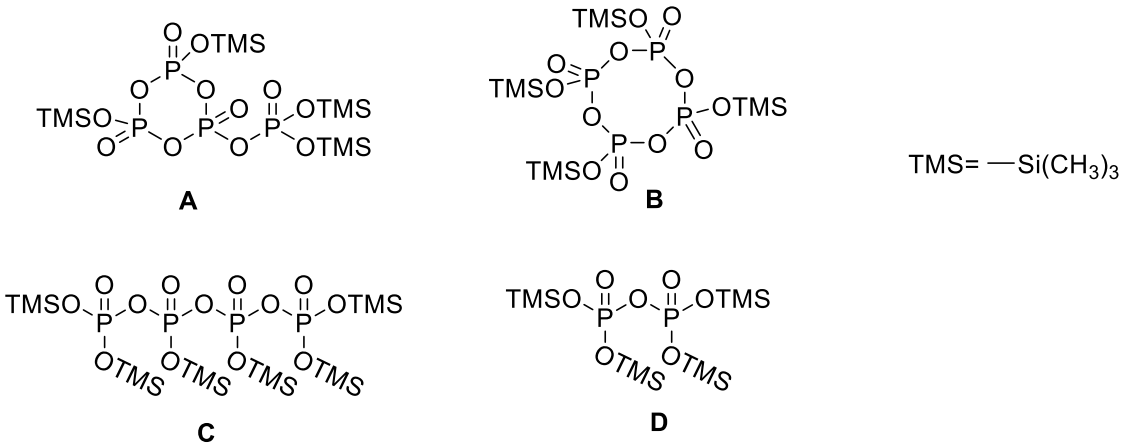

Figure 8. PPSE active species: A) isocyclotetraphosphate, B) cyclotetraphosphate, C) linear tetraphosphate, D) pyrophosphate [14]

After heating the phosphorous pentoxide and hexamethyldisiloxane to reflux for 1 hour under nitrogen, any volatile components including DCM and unreacted siloxane were distilled off at 160 °C. The resulting PPSE reagent was a viscous tan liquid, which was used for the next synthetic step.

To the obtained viscous syrup, one equivalent of the respective carboxylic acid and 2 equivalents of amine were added at 160 °C (Scheme 2). Based on the mechanism proposed by Kakimoto et al., it is thought that PPSE reacts first with the carboxylic acid to produce a mixed anhydride. While PPSE can also react with the amine, performing the reaction at high temperature (160 °C) results in the decomposition of any phosphoric amide product back to the initial amidine, preventing side reactions. Reaction of the mixed anhydride with the amide and PPSE results in a series of phosphorylated intermediates. Dephosphorylation results in formation of an imidate intermediate that can react with the amine to produce the final amidine product. [14] To collect the final amidine, the reaction was added to KOH and stirred for thirty minutes. The product was then recrystallized from a DCM/pentane mixture at -20 °C. While crystallization was observed after 24 hours, the amidine yields could be increased by leaving the solution at -20 °C for closer to 48 hours.

The carboxylic acid source used in these reactions was varied to produce amidines with different groups in the *para* position. This would result in the synthesis of model imidazolium substrates with varying Lewis acid strengths. For example, the use of 4-Br-benzoic acid will produce an amidine, and eventually an imidazolium, with a Br atom in the *para* position. Since Br is a strong electron-withdrawing group, it produced an imidazolium that was a strong Lewis acid. Addition of 4-methoxybenzoic acid on the other hand, resulted in an electron donating OMe group in the *para* position, making the final imidazolium less Lewis acidic. The amine (2,6-difluoroaniline) used in this synthesis was the same for all reactions.

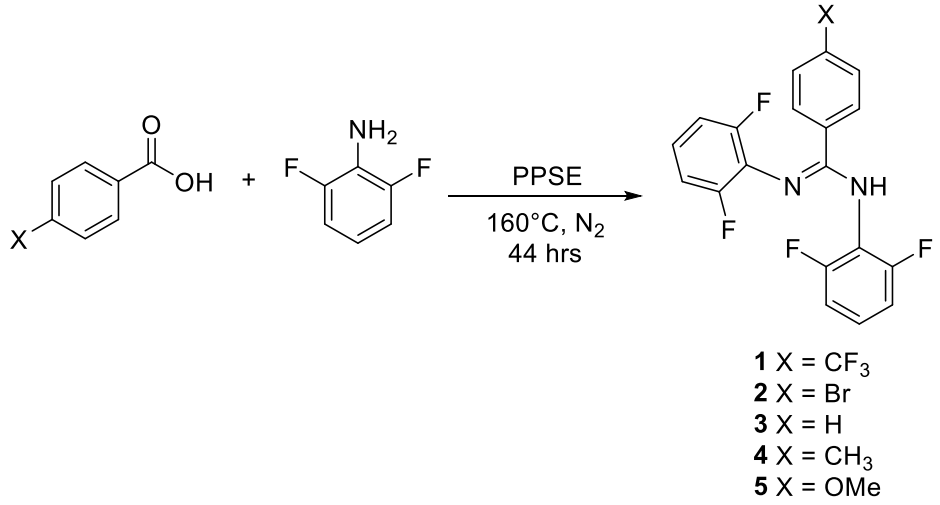

1 X = CF_3
2 X = Br
3 X = H
4 X = CH_3
5 X = OMe

Scheme 2. Synthesis of amidines using PPSE reagent, carboxylic acid, and aniline

After structural confirmation by ^{1}H and ^{19}F NMR spectroscopies, the resulting amidine was treated with 1,2-dibromoethane for 52 hours at 135 °C, based on the procedure from Meyer et al (Scheme 3). This reaction results in closing of the imidazole ring through alkylation with 1,2-dibromoethane and elimination of HBr. Reaction of a haloalkane to produce a cyclic heterocycle has been previously demonstrated in the preparation of not only imidazoliums, but other imidazole derivatives.[16] After heating for just over 2 days, the unreacted dibromoethane was removed in vacuo and the crude product dissolved in DCM. After washing with sodium bicarbonate, the organic phase was concentrated. The desired imidazolium salt could then be precipitated upon

addition of Et_2O. Removal of the ether layer and collection of the product after washing with Et_2O gave reasonably pure products. However, recrystallization at room temperature for a few hours by layering DCM/Et_2O was found to increase the purity of the product.

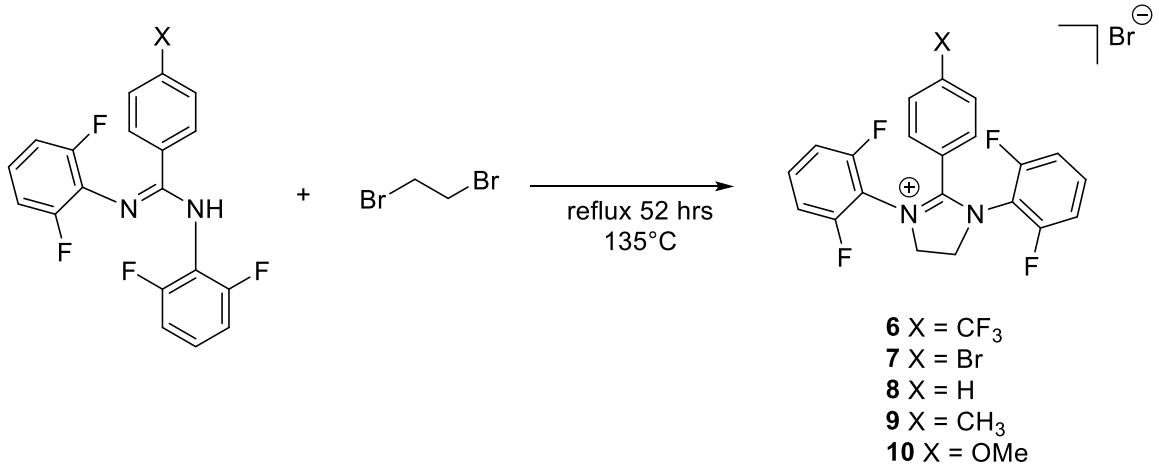

Scheme 3. Synthesis of imidazolium from synthesized amidine and 1,2-dibromoethane

One unique aspect of this reaction is that it occurs without any additional solvent. The added 1,2-dibromoethane, a liquid, acts as both a reagent and solvent. Additionally, the amidine starting material also serves as a base in this reaction, so the maximum yield is 50%. It is hypothesized that addition of a different base such as ethyldiisopropylamine, which was used in similar reactions, could help increase the final yields.[12] Of the prepared imidazolium compounds, only the methyl substituted product was previously known. Through the use of other *para* substituted carboxylic acid derivatives, new amidine and imidazolium products were synthesized (Table 1).

Table 1. Yields of the amidine and imidazolium derivatives based on their corresponding carboxylic acid precursor. The maximum yield for the imidazolium compounds is 50% because half of the amidine starting material serves as a base in the reaction.

Carboxylic Acid	Imidazolium	Amidine Yield	Imidazolium yield
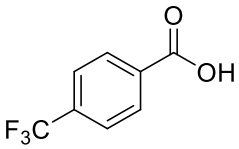	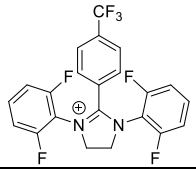	62%	17%
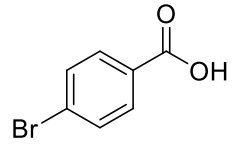	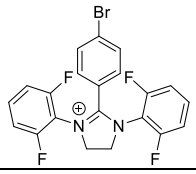	89%	34%
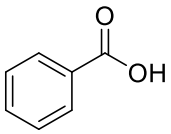	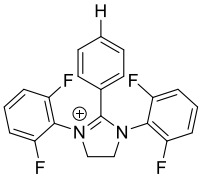	69%	20%
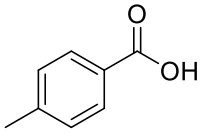	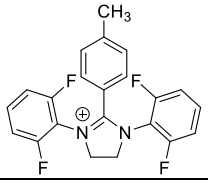	62%	31%
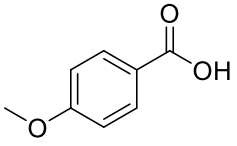	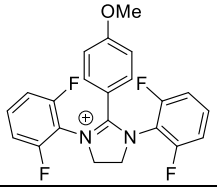	73%	20%

II. Imidazolium Reactivity based on Lewis Acidity

Meyer et al. demonstrated catalytic H_2 activation with a ruthenium-based [Fe] hydrogenase model using the CH_3-imidazolium substrate. However, their model lacked similarity to the natural enzyme in that it had a Ru center (not Fe) and no nitrogen or sulfur containing ligands.[12] It was hypothesized that using an imidazolium substrate similar to the Meyer group with a more closely related [Fe]- hydrogenase model would more accurately model the natural enzyme.

The main reason for synthesizing the *para*-substituted imidazolium derivatives was for use in the study of the model complex reactivity. As stated in the introduction, the [Fe]-carbamoyl model complex was capable of abstracting a hydride from the carbon atom of the imidazolidine substrate (Im-H). However, the reverse reaction in which the Fe center transfers the hydride back to the cationic imidazolium substrate was not observed. One reason could be that the original substrate used (CH_3-imidazolium) was not a strong enough hydride acceptor to take the hydride back from the Fe center. Therefore, by synthesizing the imidazolium derivatives described above, the Lewis acidity (and therefore hydride accepting ability) of the substrate could be tuned.

A second factor that may have been inhibiting hydride transfer to the carbocation of the imidazolium was the Lewis acidity/basicity of the model complex. While the natural enzyme has the rest of the protein environment to assist in tuning its acidity, the model Fe-carbamoyl complex lacks this flexibility. Therefore, altering the structure of the model complex may also be beneficial to observe hydride abstraction. For this reason, further studies were completed with the Fe-acyl complex, which is similar to the Fe-carbamoyl complex except that it possesses a CH_2 group in place of the NH group. From initial experiments done with the Fe-acyl complex, it was discovered that when reacted with a base (phenolate) the CH_2 group of the Fe-acyl compound is deprotonated (Scheme 4).[8]

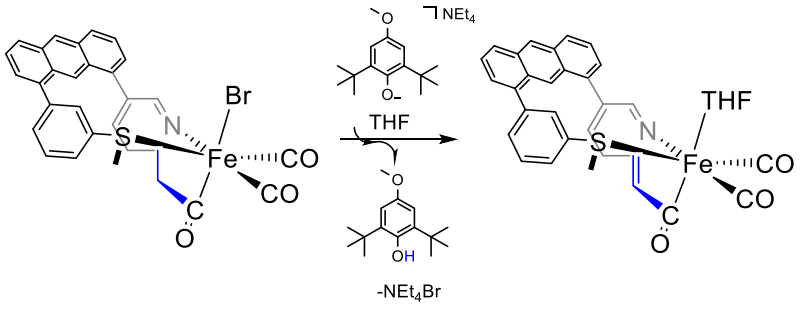

Scheme 4. Deprotonation of Fe-acyl CH_2 in the presence of phenolate base

Reactivity studies of the Fe-acyl model complex with the imidazolium derivatives are ongoing. However, some preliminary results have been obtained. Many of the reactivity results presented heretoforward were obtained by a postdoc in our group, Dr. Jun Seo. They are included as a critical component to understand the purpose and implications of the functional studies performed with the imidazolium derivatives. One important discovery is that the imidazolium is necessary to stabilize the Fe-acyl complex in the presence of D2 (or H_2) gas. Without the imidazolium, decomposition of the complex is observed (Scheme 5). The reactions in Scheme 5 demonstrate the stabilization by the imidazolium. When the imidazolium is present, an O-D (5.58 ppm), D_2 (4.52 ppm), and two THF peaks (3.58, 1.73 ppm) are observed in the ^{2}H NMR. There is also an Fe-D signal (-14.89 ppm), indicating an interaction with the Fe center. In the absence of the imidazolium substrate the O-D (5.77 ppm), D_2 (4.53 ppm), and two THF signals (3.58 and 1.73 ppm) are still present. However, an additional feature at 2.01 ppm and lack of an Fe-D resonance indicate decomposition of the Fe-acyl complex after the acyl C-C bond has dissociated. Decomposition was also confirmed using IR spectroscopy, which showed a shift in the carbonyl stretching frequencies (not shown). Overall, this data suggests that the imidazolium substrate is essential not only for H_2 activation, but also to stabilize the hydride adduct of the model complex. Therefore, H_4MPT^+ most likely plays a more important role in H_2 activation by mono-[Fe] hydrogenase and stabilization of the intermediate iron-hydride species than initially suspected.

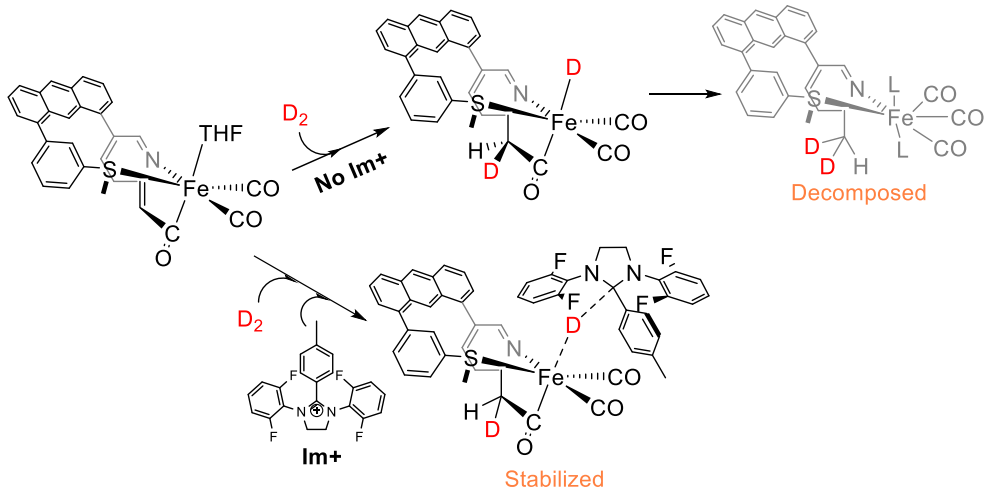

Scheme 5. Inclusion of imidazolium (bottom) in the reaction helps stabilize the Fe-acyl complex and prevents decomposition (top). D_2 gas was utilized instead of H_2 because it behaves the same way but is easier to track through NMR.

In the reaction depicted in Scheme 5, no base was added to the reaction after addition of the imidazolium substrate. This resulted in the deuteride (D^-) from D_2 going to form Fe-D, while D^+ protonated the previously formed double bond. While this was beneficial to observe Fe-D formation, transfer of the deuteride to the imidazolium substrate (Im-D) was still not observed. In order to push the reaction further in an attempt to observe Im-D formation, additional phenolate base was added (Figure 9). The ^2H NMR data collected from this reaction shows the previously observed THF, D_2, and Fe-D (-14.90 ppm) signals, but also has new peaks at 6.12 ppm and 5.58 ppm. These correspond to Im-D and phenol O-D respectively. From these results, it can be concluded that addition of the phenolate base to the reaction was successful in promoting transfer of the deuteride to the substrate. It is hypothesized that the phenolate interacts with D^+ from D_2, while the imidazolium and Fe center interact with D^-. When the phenolate abstracts D^+ to form phenol (O-D), it encourages transfer of the deuteride to the substrate, thus forming Im-D.

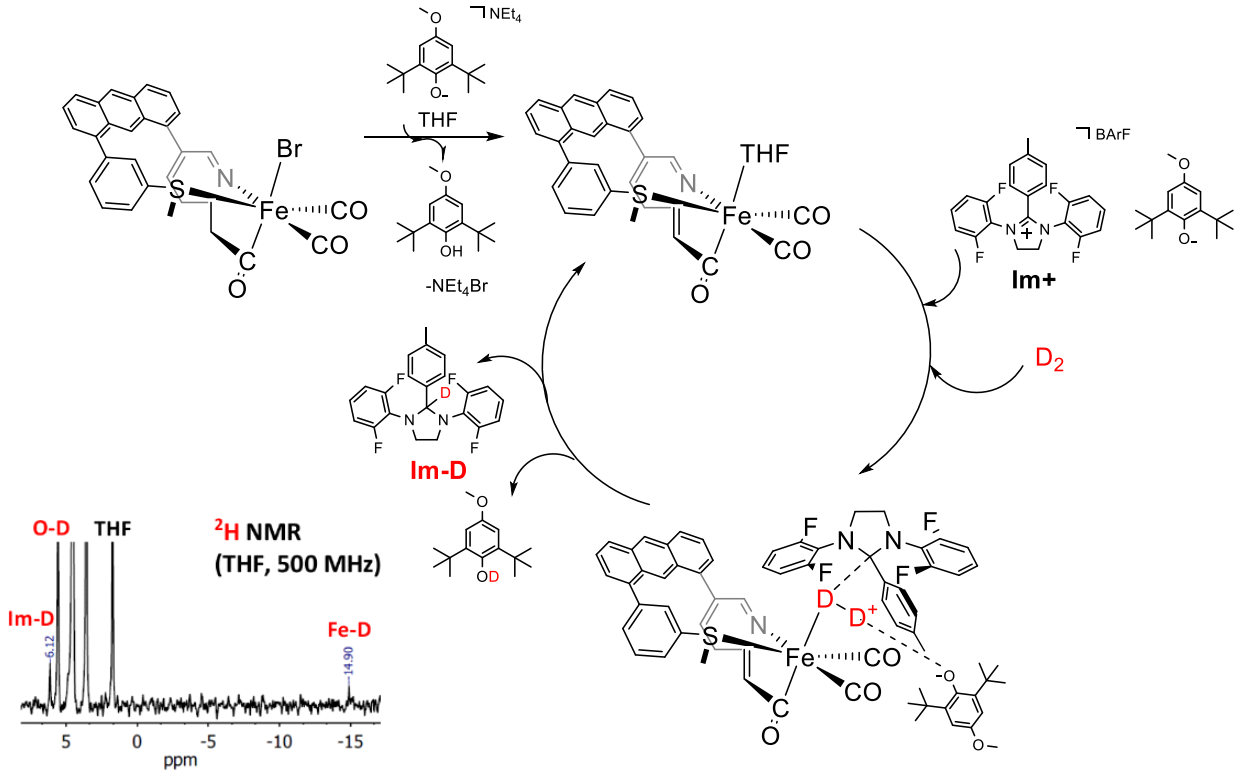

Figure 9. Reaction of Im+ phenolate base with the model Fe complex. Im-D, Fe-D, and OD signals are observed in ^{2}H NMR suggesting partial transfer of the hydride to the substrate.

While addition of base allowed for observation of the Im-D signal by ^{2}H NMR, the presence of the Fe-D signal indicates that a complete transfer of D^- to the substrate did not occur. In order to prove that the model complex is catalytic like the enzyme, full transfer to the substrate is desired. As stated earlier, changing the Lewis acidity to make the substrate a stronger hydride/deuteride acceptor was one proposed solution. Therefore, a similar reaction to Figure 9 was pursued, but instead using the CF_3-imidazolium in place of CH_3-imidazolium. Since CF_3 is a strong electron-withdrawing substituent, it draws negative charge towards the CF_3 group, making the carbocation have a stronger positive charge. This makes the overall imidazolium a stronger Lewis acid and theoretically more likely to abstract a hydride. However, results from this study indicated that CF_3 may have been too strong of a Lewis acid or preferred some other reaction, as no Fe-D or Im-D was observed in the NMR (Figure 10). Similar data was obtained for Br, a slightly

less electron-withdrawing substituent than CF_3. Based on this data it was hypothesized that an imidazolium with a Lewis acidity between CH_3-imidazolium and Br-imidazolium would work best.

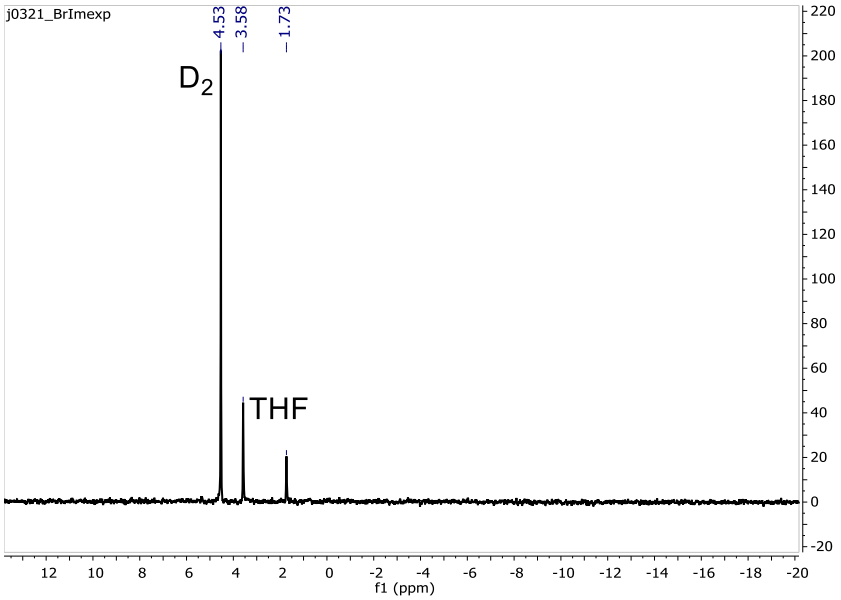

Figure 10. Reactions of the model complex with CF_3-imidazolium and Br-imidazolium model substrates. The lack of an Im-D peak suggests that hydride transfer to the substrate did not occur.

One compound that falls within this range is H-imidazolium. Compared to the electron-donating methyl group and the electron withdrawing bromo group, a proton falls in between. Due to its intermediate electronic properties, it was expected that H-imidazolium would have an ideal Lewis acidity (between Br- and CH_3-imidazolium) to promote full transfer of the deuteride from the Fe center. Figure 11 shows the ^2H NMR for the reaction. And indeed, signals at 6.13 ppm and 5.81 ppm are indicative of Im-D and the phenol O-D respectively. These indicate transfer of the hydride to the imidazolium substrate was successful. The important detail, however, is that there is no Fe-D peak observed around -15 ppm as seen in the previous NMR spectra. This suggests that transfer to H-imidazolium was successful, resulting in formation of the desired imidazolidine product. However, there is an additional signal at 4.82 ppm that requires identification before making a firm conclusion. A current hypothesis is that the H-imidazolium may have been

contaminated with some amidine, which then reacted with the deuterium in this experiment. The H-imidazolium is thus being re-crystallized to ensure its purity. After purification, this experiment will be repeated to see if the 4.82 ppm resonance will be eliminated.

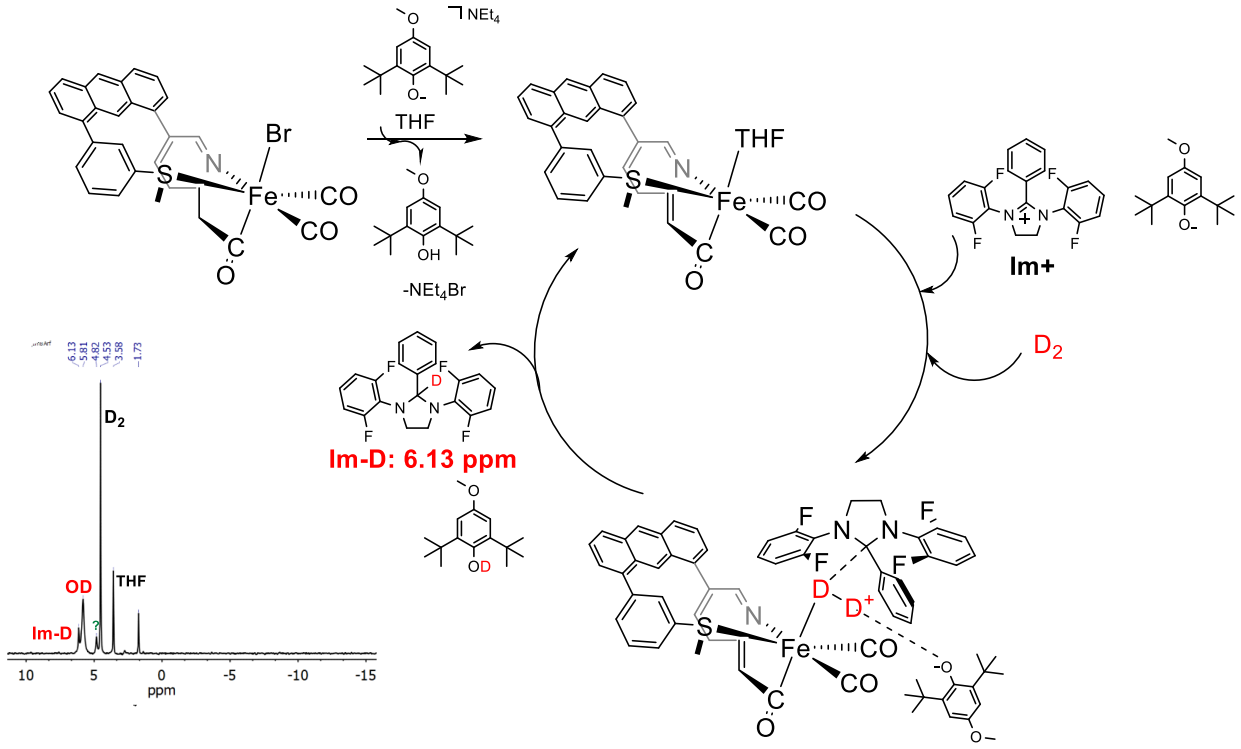

Figure 11. The reaction of the Fe-acyl model complex with H-Imidazolium led to the disappearance of the Fe-D signal. The presence of both an Im-D and OD peak suggest complete transfer of the hydride to the substrate may have occurred.

III. Imidazolium as both a Ligand and Substrate

In order to carry out the reactivity studies with the Fe-hydrogenase model complexes, the reactions must be performed in high pressure NMR tubes and the imidazolium and base must be added to the reaction. While these studies have proven useful in determining what species are present in the reaction, the precise interactions of the complex and substrate must be inferred. In order to determine the structural interactions between the complex and substrate, it would be ideal to have a crystal structure of both components interacting. To achieve this goal, it was

hypothesized that the imidazolium substrate could be covalently positioned close to the Fe center. This could allow for easier "co-crystallization" as well as additional reactivity studies.

The initial goal was to attach the imidazolium substrate to the Fe complex through a phosphine (PPh_2) bridge. This will position the substrate close to the Fe center, while still allowing some flexibility to react with H_2 (or D_2) (Figure 12).

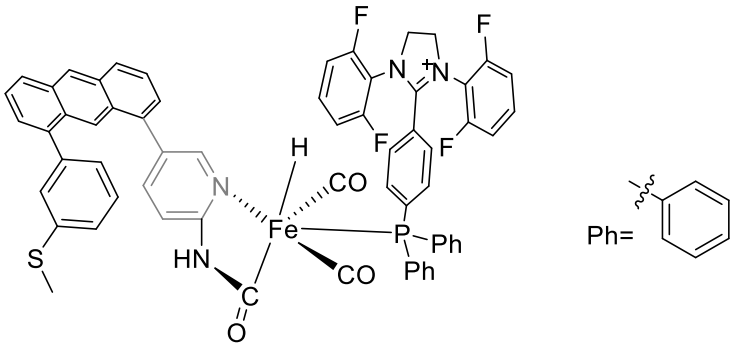

Figure 12. Phosphine-substrate model that positions the substrate close to the Fe center. The imidazolium serves as both a substrate and ligand.

One benefit of this approach is that it is a modification to an existing model complex. Either the Fe-acyl or Fe-carbamoyl complex can be used, so there is no need for the synthesis of a novel anthracene-based ligand or model complex. However, the imidazolium-phosphine ligand did require a novel preparation. This was carried out by a 4-step procedure. The first two steps involved synthesis of the Br-imidazolium complex from 4-Br-benzoic acid and 2,6-difluoroaniline (described in Scheme 2 and 3 above). The third step converted the Br-benzoic acid bromide salt to a BArF (Tetrakis[3,5-bis(trifluoromethyl)phenyl]borate) salt (Scheme 6). This made it possible to carry out the subsequent lithiation reaction since the Br counterion may have reacted with the lithium ions instead of the Br on the imidazolium. Conversion to the BArF salt also helped increase solubility.

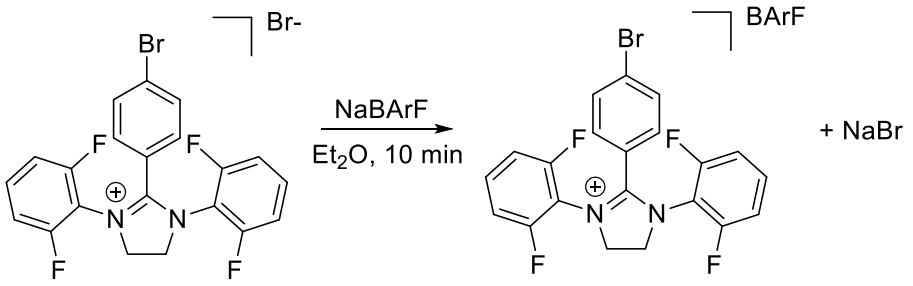

Scheme 6. Conversion of Br-imidazolium bromide salt into BArF salt

The fourth step utilized the functionality of the Br group to attach diphenylphosphine in the *para* position (Scheme 7). In this reaction, the Br group on the imidazolium was first lithiated using n-butyllithium. A color change from yellow to a dark orange was observed. Upon addition of the phosphine source, $ClPPh_2$, the reaction turned back to yellow. After extractions with Et_2O, the resulting product is a yellow-white powder.

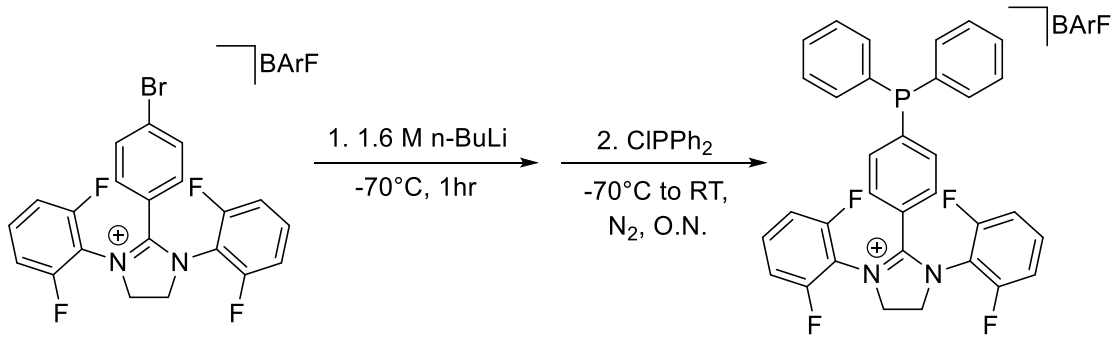

Scheme 7. Attachment of PPh_2 to Br-imidazolium through lithiation and subsequent addition of a phosphine source

This phosphine-imidazolium product has been successfully synthesized but has not yet been purified. From the resulting mass spectrometry analysis, the major impurity appears to be H-imidazolium. This suggests that the lithiation step is successful, but attachment of PPh_2 is not complete. Increasing the $ClPPh_2$ source to 2 equivalents was unsuccessful at improving purity. As the product is air-sensitive, purification by a column is difficult. Therefore, changing the stoichiometry of the reactants and modifying the work-up procedure seem to be the next steps for obtaining a purer product. After purification, metalation with the Fe-acyl or Fe-carbamoyl complex

will be carried out. From there the product can be used for reactivity or X-ray studies to elucidate the structural interactions that occur between the model complex and the imidazolium substrate.

Conclusion

In summary, based on this preliminary data, when the Fe-acyl model was combined with a model imidazolium substrate of an ideal Lewis acidity, transfer of a hydride to the model substrate was observed. Additionally, it was determined that the model substrate helped stabilize the iron-hydride intermediate during the reaction. These results suggest that the Lewis acidity of the natural methenyl-H_4MPT^+ substrate and mono-[Fe] hydrogenase plays an important role in H_2 activation. Reactivity studies with the imidazolium derivatives are currently ongoing, as well as structural studies to covalently position the substrate close to the iron complex. Future goals include incorporating a pyridone and/or thiolate donor into the ligand backbone to more closely model the naturally occurring mono-[Fe] hydrogenase enzyme.

Materials and Methods

All reactions were carried out under N_2 using standard Schlenk line and glovebox techniques. The included ^1H and ^{19}F NMR spectra were collected using a Varian DirectDrive 400 instrument. All ^{31}P NMR were collected using an Agilent MR 400 instrument.

Synthesis

***N*,*N*-bis(2,6-difluorophenyl)-4-(trifluoromethyl)benzamidine (1)**

Phosphorous pentoxide (15.2 g, 53.7 mmol, 6 eq.) and hexamethyldisiloxane (24.7 mL, 116 mmol, 13 eq.) were prepared in a 250 mL Schlenk flask. DCM (30 mL) was added in the glovebox and the solution was heated to reflux for 1 h under N_2. The DCM and any unreacted hexamethyldisiloxane were then removed by distillation at 160 °C. To the remaining solution, 4-

trifluoromethylbenzoic acid (1.70 g, 8.94 mmol, 1 eq.) and 2,6-difluoroaniline (2.41 mL, 22.3 mmol, 2.5 eq.) were added and the reaction was stirred at 160 °C for 42 hrs. While still hot, the viscous tan solution was added to an aqueous solution of KOH (400 mL, 0.5 M) and stirred vigorously for 1 h. The mixture was then extracted with DCM (3 x 100 mL), the organic layer dried over Na_2SO_4, and then filtered over neutral aluminum oxide. The solution volume was reduced in vacuo and pentane (50 mL) was added to the solution. After storing the solution at -20 °C for 48 hrs, white crystals were collected by filtration. Washing with pentane afforded 2.28 g of white powder (62%). ^{1}H NMR (400 MHz, $CDCl_3$): δ (ppm) = 7.87 (1 H), 7.56 (3 H), 6.99 (2 H), 6.83 (4 H), 6.11 (1 H). ^{19}F NMR ($CDCl_3$): δ (ppm) = -63.02 (s), −119.5 (s), −121.5 (s). HR-MS (ESI-MS): Calcd. for $[C_{20}H_{11}F_7N_2+H]+$ 413.08830; found: 413.08980.

4-bromo-N,N'-bis(2,6-difluorophenyl)benzamidine (2)

Phosphorous pentoxide (14.4 g, 50.8 mmol, 6 eq.) and hexamethyldisiloxane (23.4 mL, 110 mmol were prepared in a 250 mL Schlenk flask. DCM (30 mL) was added in the glovebox and the solution was heated to reflux for 1 h under N_2. The DCM and any unreacted hexamethyldisiloxane were then removed by distillation at 160 °C. To the remaining solution, 4-bromobenzoic acid (1.70 g, 8.46 mmol, 1 eq.) and 2,6-difluoroaniline (2.28 mL, 21.2 mmol, 2.5 eq.) were added and the reaction was stirred at 160 °C for 44 hrs. While still hot, the viscous tan solution was added to an aqueous solution of KOH (400 mL, 0.5 M) and stirred vigorously for 1 h. The mixture was then extracted with DCM (3 x 100 mL), the organic layer dried over Na_2SO_4, and then filtered over neutral aluminum oxide. The solution volume was reduced in vacuo and pentane (50 mL) was added to the solution. After storing the solution at -20 °C for 48 hrs, white crystals were collected by filtration. Washing with pentane afforded 3.19 g of white powder (89 %). ^{1}H NMR (400 MHz, $CDCl_3$): δ (ppm) = 7.60 (1 H), 7.52 (1 H), 7.42 (d, 2 H), 6.99 (s, 3 H), 6.83 (m, 4 H). ^{19}F NMR

($CDCl_3$): δ (ppm) = −119.58 (s), −121.53 (s). HR-MS (ESI-MS): Calcd. for $[C_{21}H_{14}F_7BrF_4N_2+H]+$ 449.02710; found: 449.0285.

N,N'-bis(2,6-difluorophenyl)benzamidine (3)

Phosphorous pentoxide (17.8 g, 62.7 mmol, 6 eq.) and hexamethyldisiloxane (29.0 mL, 137 mmol, 13 eq.) were prepared in a 250 mL Schlenk flask. DCM (30 mL) was added in the glovebox and the solution was heated to reflux for 1 h under N_2. The DCM and any unreacted hexamethyldisiloxane were then removed by distillation at 160 °C. To the remaining solution, benzoic acid (1.28 g, 10.5 mmol, 1.0 eq.) and 2,6-difluoroaniline (2.82 mL, 26.25 mmol, 2.5 eq.) were added and the reaction was stirred at 160 °C for 44 hrs. While still hot, the viscous tan solution was added to an aqueous solution of KOH (400 mL, 0.5 M) and stirred vigorously for 1 h. The mixture was then extracted with DCM (3 x 100 mL), the organic layer dried over Na_2SO_4, and then filtered over neutral aluminum oxide. The solution volume was reduced in vacuo and pentane (50 mL) was added to the solution. After storing the solution at -20 °C for 24 hrs, white crystals were collected by filtration. Washing with pentane afforded 2.49 g of white powder (69%).

N,N'-bis(2,6-difluorophenyl)-4-methylbenzamidine (4)

Synthesis of this compound was carried out using the procedure from Meyer et al.[12] Phosphorous pentoxide (21.3 g, 75.0 mmol, 6 eq.) and hexamethyldisiloxane (34.2 mL, 160 mmol, 13 eq.) were prepared in a 250 mL Schlenk flask. DCM (30 mL) was added in the glovebox and the solution was heated to reflux for 1 h under N_2. The DCM and any unreacted hexamethyldisiloxane were then removed by distillation at 160 °C. To the remaining solution, *p*-toluic acid (1.70 g, 12.5 mmol, 1.0 eq.) and 2,6-difluoroaniline (3.39 mL, 31.4 mmol, 2.5 eq.) were added and the reaction was stirred at 160 °C for 40 hrs. While still hot, the viscous tan solution was added to an aqueous solution of KOH (400 mL, 0.5 M) and stirred vigorously for 1 h. The mixture was then extracted

with DCM (3 x 100 mL), the organic layer dried over Na_2SO_4, and then filtered over neutral aluminum oxide. The solution volume was reduced in vacuo and pentane (50 mL) was added to the solution. After storing the solution at -20 °C for 24 hrs, white crystals were collected by filtration. Washing with pentane afforded 2.77 g of white powder (62 %). This product is a mixture of two isomers. Only the major isomer data is reported. ^{1}H NMR (400 MHz, $CDCl_3$): δ (ppm) = 7.30 (d, 2 H), 7.17 (d, 1 H), 7.10 (d, 2H), 6.94 (m, 2 H), 6.84–6.76 (m, 3 H), 6.16 (s, 1 H), 2.31 (s, 3 H). ^{19}F NMR ($CDCN_3$): δ (ppm) = −119.57 (s), −121.63 (s). HR-MS (ESI-MS): Calcd. for $[C_{20}H_{14}F_4N_2+H]+$ 359.11660; found: 359.11690.

N,N'-bis(2,6-difluorophenyl)-4-methoxybenzamidine (5)

Phosphorous pentoxide (19.1 g, 67.2 mmol, 6 eq.) and hexamethyldisiloxane (30.9 mL, 146 mmol, 13 eq.) were prepared in a 250 mL Schlenk flask. DCM (30 mL) was added in the glovebox and the solution was heated to reflux for 1 h under N_2. The DCM and any unreacted hexamethyldisiloxane were then removed by distillation at 160 °C. To the remaining solution, 4-methoxybenzoic acid (1.70 g, 11.2 mmol, 1.0 eq.) and 2,6-difluoroaniline (3.0 mL, 27.7 mmol, 2.5 eq.) were added and the reaction was stirred at 160 °C for 44 hrs. While still hot, the viscous tan solution was added to an aqueous solution of KOH (400 mL, 0.5 M) and stirred vigorously for 1 h. The mixture was then extracted with DCM (3 x 100 mL), the organic layer dried over Na_2SO_4, and then filtered over neutral aluminum oxide. The solution volume was reduced in vacuo and pentane (50 mL) was added to the solution. After storing the solution at -20 °C for 48 hrs, white crystals were collected by filtration. Washing with pentane afforded 3.05 g of white powder (73%). ^{1}H NMR (400 MHz, $CDCl_3$): δ (ppm) = 7.71 (d, 1 H), 7.37 (d, 2 H), 6.95 (m, 2 H), 6.88–6.78 (m, 8 H), 6.05 (s, 1 H), 3.77 (s, 3 H). ^{19}F NMR ($CDCl_3$): δ (ppm) = -119.73, -121.69. HR-MS (ESI-MS): Calcd. for $[C_{20}H_{14}F_4N_2O+H]+$ 375.11150; found: 375.11170.

1,3-bis(2,6-difluorophenyl)-2-(4-(trifluoromethyl)phenyl)-4,5-dihydro-1*H*-imidazol-3-ium Bromide (6)

1,2-dibromoethane (5 mL) was added to a Schlenk flask containing *N*,*N*-bis(2,6-difluorophenyl)-4-(trifluoromethyl)benzamidine (1.0 g, 2.4 mmol) and the reaction was heated to reflux for 58 hrs. After removing the solvent in vacuo, the crude solid was dissolved in DCM (15 mL) and washed with aqueous $NaHCO_3$ (15 mL). The organic layer was extracted with DCM (3x15 mL), dried over Na_2SO_4, and concentrated in vacuo. Addition of Et_2O (5 mL) precipitated a tan solid that was collected by decanting the Et_2O layer and washing the solid with Et_2O (3x3 mL). The product was recrystallized at room temperature by layering DCM/Et_2O (5 mL/ 5 mL) to afford 0.182 g (17%) of light yellow solid. The remaining Et_2O layer contains unreacted benzamidine. ^{1}H NMR (400 MHz, CD_3CN): δ (ppm) = 7.58 (d, 2 H), 7.50–7.42 (m, 4 H), 7.07-7.02 (m, 4 H), 4.62 (s, 4 H). ^{19}F NMR (CD_3CN): δ (ppm) = -64.28 (s), −118.01 (s). HR-MS (ESI-MS): Calcd. for $[C_{22}H_{14}F_7N_2+H]+$ 439.10400; found: 439.10520.

2-(4-bromophenyl)-1,3-bis(2,6-difluorophenyl)-4,5-dihydro-1*H*-imidazol-3-ium Bromide (7)

1,2-dibromoethane (5 mL) was added to a Schlenk flask containing 4-bromo-N,N'-bis(2,6-difluorophenyl)benzamidine (1.0 g, 2.4 mmol) and the reaction was heated to reflux for 56 hrs. After removing the solvent in vacuo, the crude solid was dissolved in DCM (15 mL) and washed with aqueous $NaHCO_3$ (15 mL). The organic layer was extracted with DCM (3x15 mL), dried over Na_2SO_4, and concentrated in vacuo. Addition of Et_2O (5 mL) precipitated a tan solid that was collected by decanting the Et_2O layer and washing the solid with Et_2O (3x3 mL). The product was recrystallized at room temperature by layering DCM/Et_2O (5 mL/ 5 mL) to afford 0.363 g (34%) of tan solid. The remaining Et_2O layer contains unreacted benzamidine. ^{1}H NMR (400 MHz, CD_3CN): δ (ppm) = 7.59-7.55 (m, 4 H), 7.24 (d, 2 H), 7.18-7.13 (m, 4 H), 4.68 (s, 4 H).^{19}F NMR

(CD_3CN): δ (ppm) = −118.2. HR-MS (ESI-MS): Calcd. for $[C_{21}H_{14}BrF_4N_2+H]+$ 449.02710; found: 449.02850.

1,3-bis(2,6-difluorophenyl)-2-phenyl-4,5-dihydro-1*H*-imidazol-3-ium Bromide (8)

1,2-dibromoethane (5 mL) was added to a Schlenk flask containing N,N'-bis(2,6-difluorophenyl)benzamidine (1.0 g, 2.9 mmol) and the reaction was heated to reflux for 52 hrs. After removing the solvent in vacuo, the crude solid was dissolved in DCM (15 mL) and washed with aqueous $NaHCO_3$ (15 mL). The organic layer was extracted with DCM (3x15 mL), dried over Na_2SO_4, and concentrated in vacuo. Addition of Et_2O (5 mL) precipitated a white solid that was collected by decanting the Et_2O layer and washing the solid with Et_2O (3x3 mL). The product was recrystallized at room temperature by layering DCM/Et_2O (5 mL/ 5 mL) to afford 0.215 g (20%) of tan solid. The remaining Et_2O layer contains unreacted benzamidine. ^{1}H NMR (400 MHz, $CDCl_3$): δ (ppm) = 7.52 (m, 1 H), 7.45-7.39 (m, 1 H), 7.32 (t, 3 H), 7.24 (1 H), 7.22 (1 H), 7.03-6.99 (m, 3 H), 5.13 (s, 4H). ^{19}F NMR ($CDCl_3$): δ (ppm) = -116.73. HR-MS (ESI-MS): Calcd. for $[C_{21}H_{15}F_4N_2+H]+$ 371.11660; found: 371.11680.

1,3-bis(2,6-difluorophenyl)-2-(*p*-tolyl)-4,5-dihydro-1*H*-imidazol-3-ium Bromide (9)

Synthesis of this compound was carried out using the procedure from Meyer et al.[12] 1,2-dibromoethane (5 mL) was added to a Schlenk flask containing N,N'-bis(2,6-difluorophenyl)-4-methylbenzamidine (1.0 g, 2.8 mmol) and the reaction was heated to reflux for 52 hrs. After removing the solvent in vacuo, the crude solid was dissolved in DCM (15 mL) and washed with aqueous $NaHCO_3$ (15 mL). The organic layer was extracted with DCM (3x15 mL), dried over Na_2SO_4, and concentrated in vacuo. Addition of Et_2O (5 mL) precipitated a tan solid that was collected by decanting the Et_2O layer and washing the solid with Et_2O (3x3 mL). The product was recrystallized at room temperature by layering DCM/Et_2O (5 mL/ 5 mL) to afford 0.422 g (39%)

of tan solid. The remaining Et_2O layer contains unreacted benzamidine. ^1H NMR (400 MHz, $CDCl_3$): δ (ppm) = 7.47-7.39 (m, 2 H), 7.10 (s, 4 H), 7.01 (t, 4 H), 5.09 (s, 4 H), 2.30 (s, 3 H). ^{19}F NMR (400 MHz): δ (ppm) = -116.84.

1,3-bis(2,6-difluorophenyl)-2-(4-methoxyphenyl)-4,5-dihydro-1*H*-imidazol-3-ium Bromide (10)

1,2-dibromoethane (5 mL) was added to a Schlenk flask containing N,N'-bis(2,6-difluorophenyl)-4-methoxybenzamidine (1.0 g, 2.7 mmol) and the reaction was heated to reflux for 52 hrs. After removing the solvent in vacuo, the crude solid was dissolved in DCM (15 mL) and washed with aqueous $NaHCO_3$ (15 mL). The organic layer was extracted with DCM (3x15 mL), dried over Na_2SO_4, and concentrated in vacuo. Addition of Et_2O (5 mL) precipitated a tan solid that was collected by decanting the Et_2O layer and washing the solid with Et_2O (3x3 mL). The product was recrystallized at room temperature by layering DCM/Et_2O (5 mL/ 5 mL) to afford 0.211 g (20%) of tan solid. The remaining Et_2O layer contains unreacted benzamidine. ^1H NMR (400 MHz, $CDCl_3$): δ (ppm) = 7.48-7.40 (m, 2 H), 7.14 (d, 2 H), 7.03 (m, 4 H), 6.79 (d, 2 H), 5.05 (s, 4 H), 3.77 (s, 3 H). ^{19}F NMR ($CDCl_3$): δ (ppm) = -116.81

1,3-bis(2,6-difluorophenyl)-2-(4-diphenylphosphaneyl)phenyl)-4,5-dihydro-1H-imidazol-3-ium BArF (11)

To a vial of 2-(4-bromophenyl)-1,3-bis(2,6-difluorophenyl)-4,5-dihydro-1*H*-imidazol-3-ium (0.100 g, 0.22 mmol, 1 eq.) in Et_2O (15 mL), NaBArF (0.195 g, 0.22 mmol, 1 eq.) dissolved in Et_2O (2 mL) was added and the mixture was stirred for 10 minutes. The precipitated NaBr was removed by filtering the light beige solution through a celite-packed pipet into a 50 mL Schlenk flask. The reaction was performed under N_2 and cooled to -70 °C in a dry ice/acetone bath. N-Butyllithium (0.14 mL, 0.22 mmol) was added dropwise to the flask and the solution stirred at -70

°C for 1 h. Upon addition of n-BuLi, the reaction changed from a light yellow to a dark orange color. Chlorodiphenylphosphine (0.04 mL, 0.22 mmol) was then added dropwise at -70 °C and the solution was allowed to slowly warm to room temperature. After stirring for 20 hrs, degassed H_2O (5 mL) was added to the reaction and stirred for 10 minutes, turning the solution from an opaque white solution to clear yellow. The Et_2O layer from the reaction flask was then transferred to a new 50 mL Schlenk flask containing Na_2SO_4 and already under a N_2 atmosphere. After a few minutes, the Et_2O layer was removed in vacuo with a cold trap. The flask was brought into the glovebox, the solid re-dissolved in Et_2O, and filtered through a celite-packed pipet. The Et_2O was removed in vacuo to yield a yellow-white solid. The NMR is reported for the major signals in the crude product as purification has been unsuccessful. ^{1}H NMR (400 MHz, $CDCl_3$): δ (ppm) = 8.65 (s), 7.72–7.63 (m), 7.59-7.55 (m), 7.50-7.43 (m), 7.15 (m) 6.92 (m), 5.28 (s), 4.53 (s). ^{19}F NMR ($CDCl_3$): δ (ppm) = -62.48, -117.85. ^{31}P NMR (400 MHz, $CDCl_3$): δ (ppm) = 22.88, -19.10, -19.39, -40.39. HR-MS (ESI-MS): Calcd. for $[C_{33}H_{24}F_4N_2P+H]+$ 555.16300; found: 555.16080.

Acknowledgements

All reactivity studies between the imidazolium and model complex were carried out by Dr. Jun Seo or Spencer Kerns. The data is included to help explain how the imidazolium derivatives are being used and their importance to H_2 activation. All reactions were carried out with the space and resources provided by Dr. Michael Rose. Thanks to the members of the Rose Group (especially hydrogenase members) for their support and assistance with this research.

References

1 Clerici, A. et al. World Energy Outlook 2013. **2013,** 6-8.

2 Office of Energy, Efficiency, & Renewable Energy. Hydrogen Production: Electrolysis. https://energy.gov/eere/fuelcells/hydrogen-production-electrolysis

3 Office of Energy, Efficiency, & Renewable Energy. Vehicle Technologies Office: Hydrogen Cost and Worldwide Production. https://energy.gov/eere/vehicles/vehicle-technologies-office-fuel-efficiency-and-emissions

4 Holladay, J. D.; Hu, J.; King, D.L.; Wang, Y. Overview of hydrogen production technologies. *Catal. Today*. **2009**, *4*, 244-260.

5 Das, D.; Dutta, T; Nath, K.; Kotay, S.; Das, A.; Veziroglu, N. Role of Fe-hydrogenase in biological hydrogen production. *Curr. Sci*. **2006**, *12*, 1627-1637.

6 Stiebritz, M.T.; Reiher, M. Hydrogenases and oxygen. *Chem. Sci*. **2012**, *6*, 1739-1751.

7 Winkler, M.; Esselborn, J.; Happe, T. Molecular basis of [Fe-Fe]-hydrogenase function: An insight into the complex interplay between protein and catalytic cofactor. *Biochim. Biophys. Acta.* **2013**, *8*, 974-985.

8 Seo, J.; Manes, T.A.; Rose, M.J. Structural and functional synthetic model of mono-iron hydrogenase featuring an anthracene scaffold. *Nat. Chem.* [Online]. **2017**.

9 Hiromoto, T.; Ataka, K.; Pilak, O.; Vogt, S.; Stagni, M.S.; Meyer-Klaucke, W.; Warkentin, E.; Thauer, R.; Shima, S.; Ermler, U. The crystal structure of C176A mutated [Fe]-hydrogenase suggests an acyl-iron ligation in the active site iron complex. *FEBS Letters*. ***2009****, 583*, 585-590.

10 Finkelmann, A.R.; Senn, H.M.; Reiher,M. Hydrogen-activation mechanism of [Fe]-hydrogenase revealed by multi-scale modeling. *Chem. Sci*. **2014**, *5*, 4474.

11 Thauer, R. K.; Kaster, A.; Goenrich, M.; Schick, M. Hiromoto, T.; Shima, S. Hydrogenases from Methanogenic Archea, Nickel, a Novel Cofactor, and H2 Storage. *Annu. Rev. Biochem*. **2010**, *79*, 507.

12 Allikmaa, V.; Eek, M.; Pehk, T.; Lopp, M. A Convenient Method for the Construction of the Imidazolone Ring in the Synthesis of Benzamidine Derivatives. *Proc. Estonian Acad. Sci. Chem.* **2001**, *3*, 180-185.

13 Meyer, F.; Kalz, K.F.; Brinkmeier, A.; Dechert, S.; Mata, R. A. Functional Model for the [Fe] hydrogenase Inspired by the Frustrated Lewis Pair Concept. *J. Am. Chem. Soc.* **2014**, *136*, 16626-16634.

14 Kakimoto, M. Imai, Y.; Ogata, S.; Mochizuki, A. Synthesis of amides and amidines by reaction of carboxylic acids and amines in the presence of polyphophoric acid trimethylsilyl ester (PPSE). *Bull. Chem. Soc. Jpn.* **1986**, *59*, 2171-2177.

15 Imamoto, T.; Matsumoto, H.Y.; Yokoyama, M.; Yamaguchi, K. Preparation and synthetic use of trimethylsilyl polyphosphate: A new stereoselective aldol-type reaction in the presence of trimethyl silyl polyphosphate. *J. Org. Chem.* **1984**, *49*, 1105-1110.

16 Zhang. H.; Yan, X.; Zhao, J.; Yang, X.; Huang, Z.; Zhou, G. Wu, Y. Synthesis of 2,2'-biimidazole-based platinum(II) polymetallaynes and turning their fluorescent response behaviors in Cu2+ ions through optimizing the configuration of the organic spacers and steric effect. *RSC Advances*. **2015**, *108*, 88758-88766.

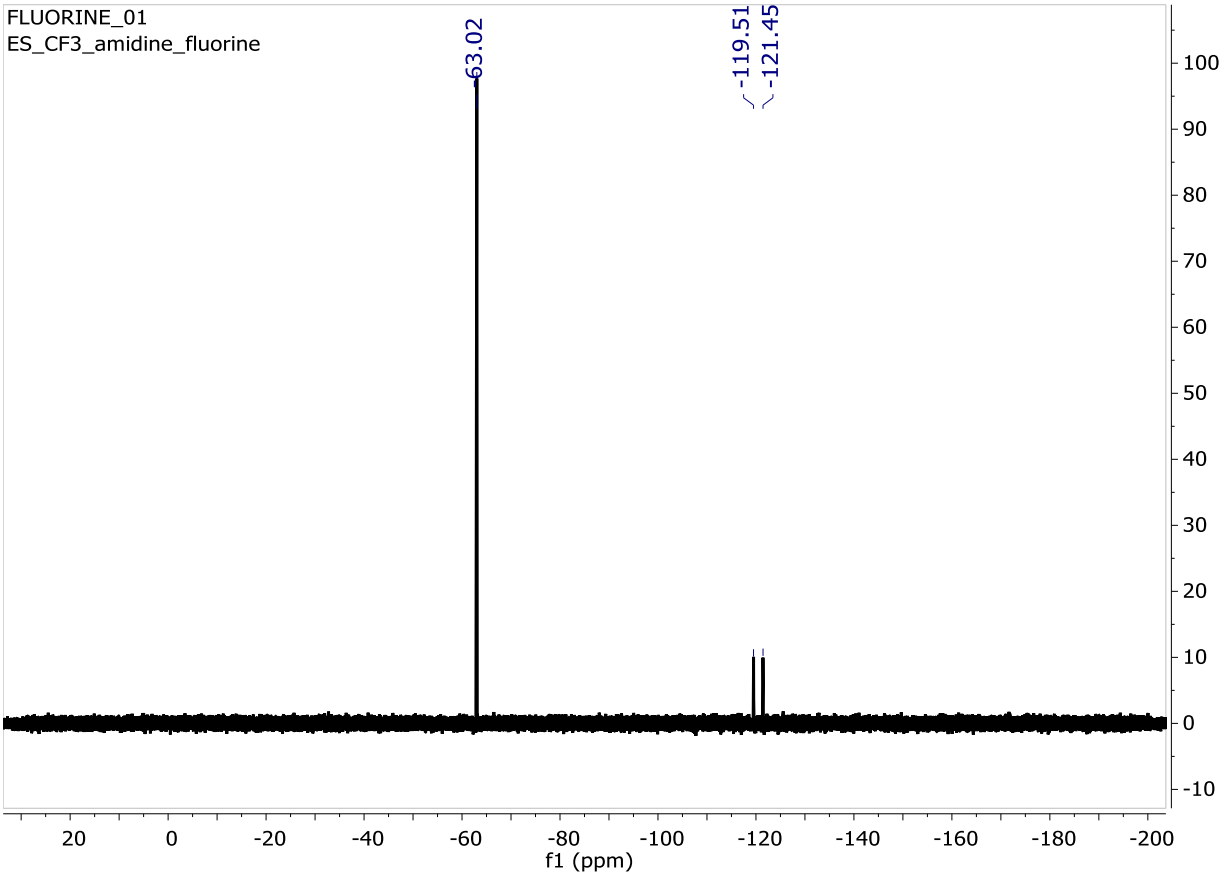

Supplementary Figure 1. ^{19}F NMR CF_3-amidine in $CDCl_3$

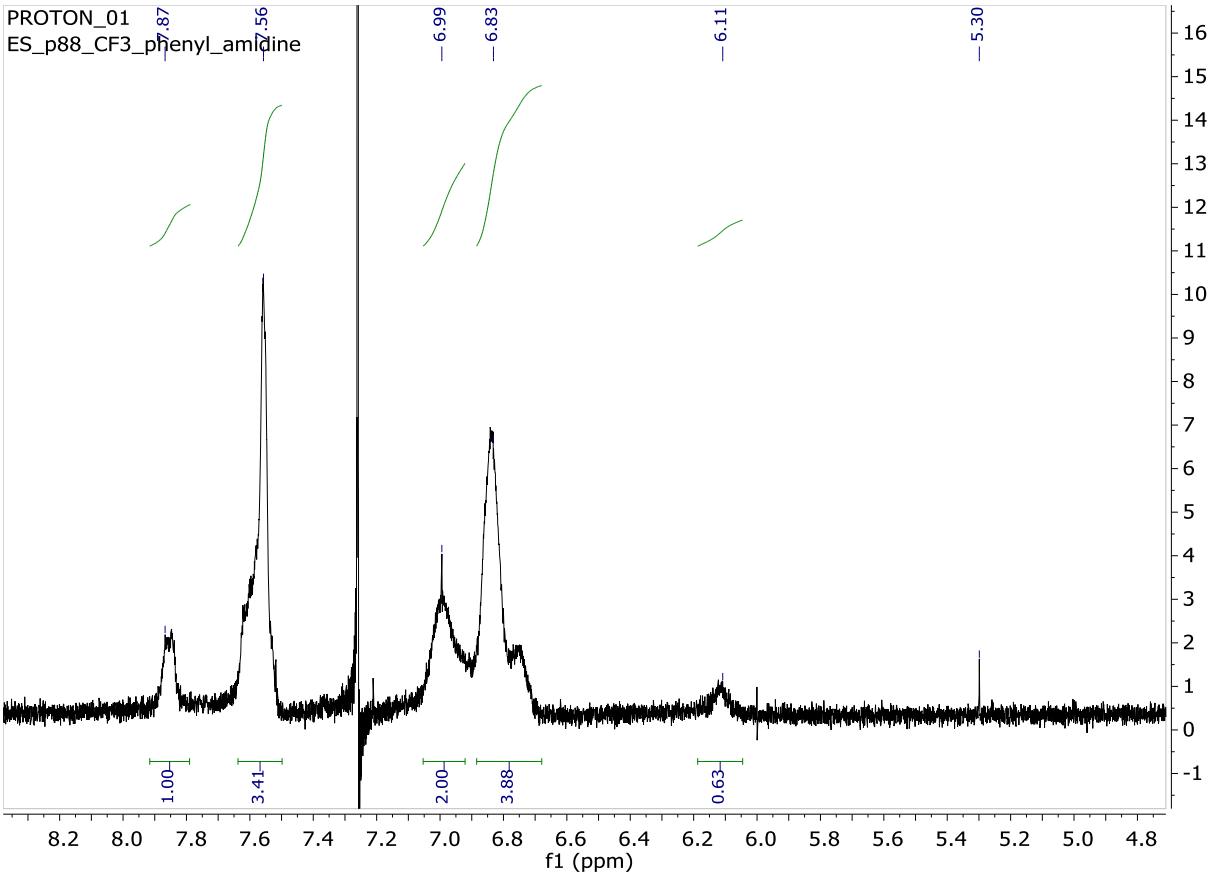

Supplementary Figure 2. ^{1}H NMR CF_3-amidine in $CDCl_3$

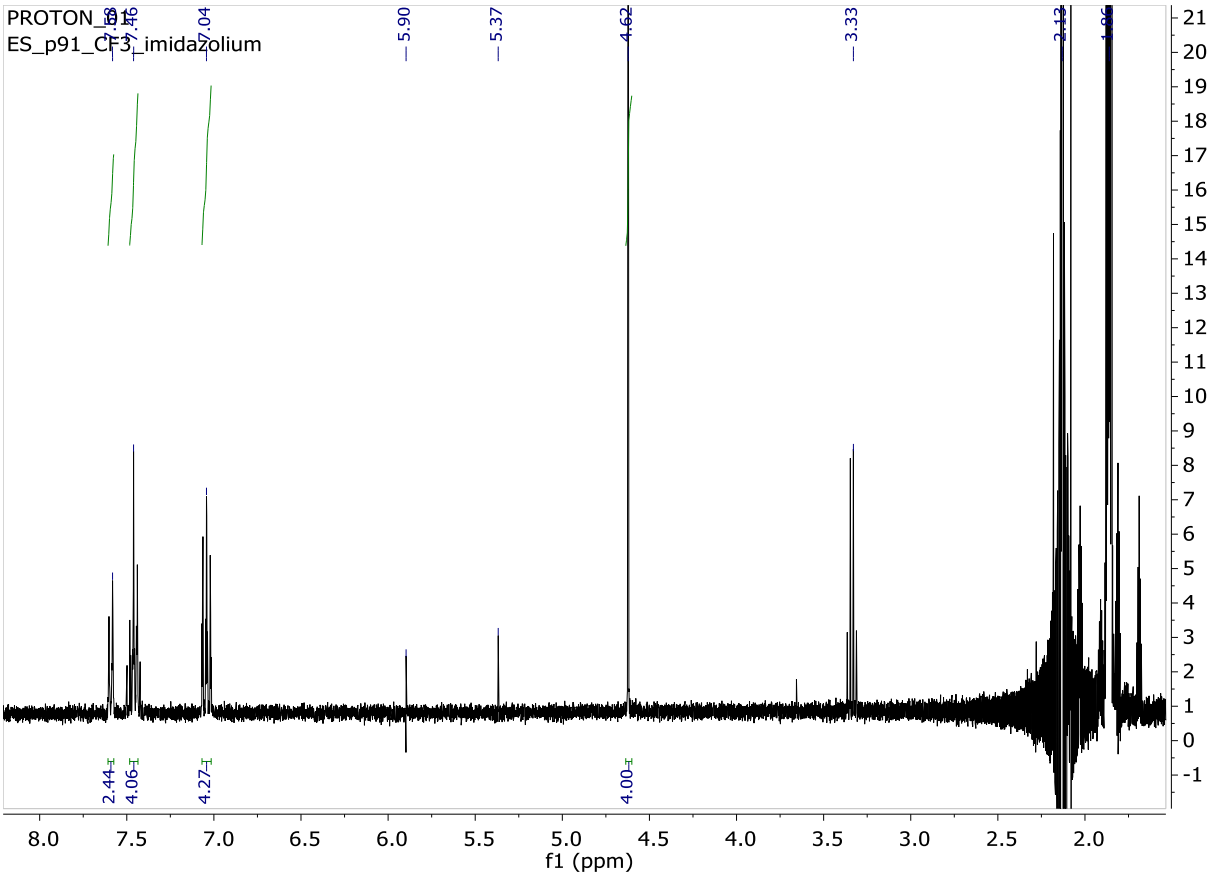

Supplementary Figure 3. ^{1}H NMR CF_3-imidazolium in CD_3CN

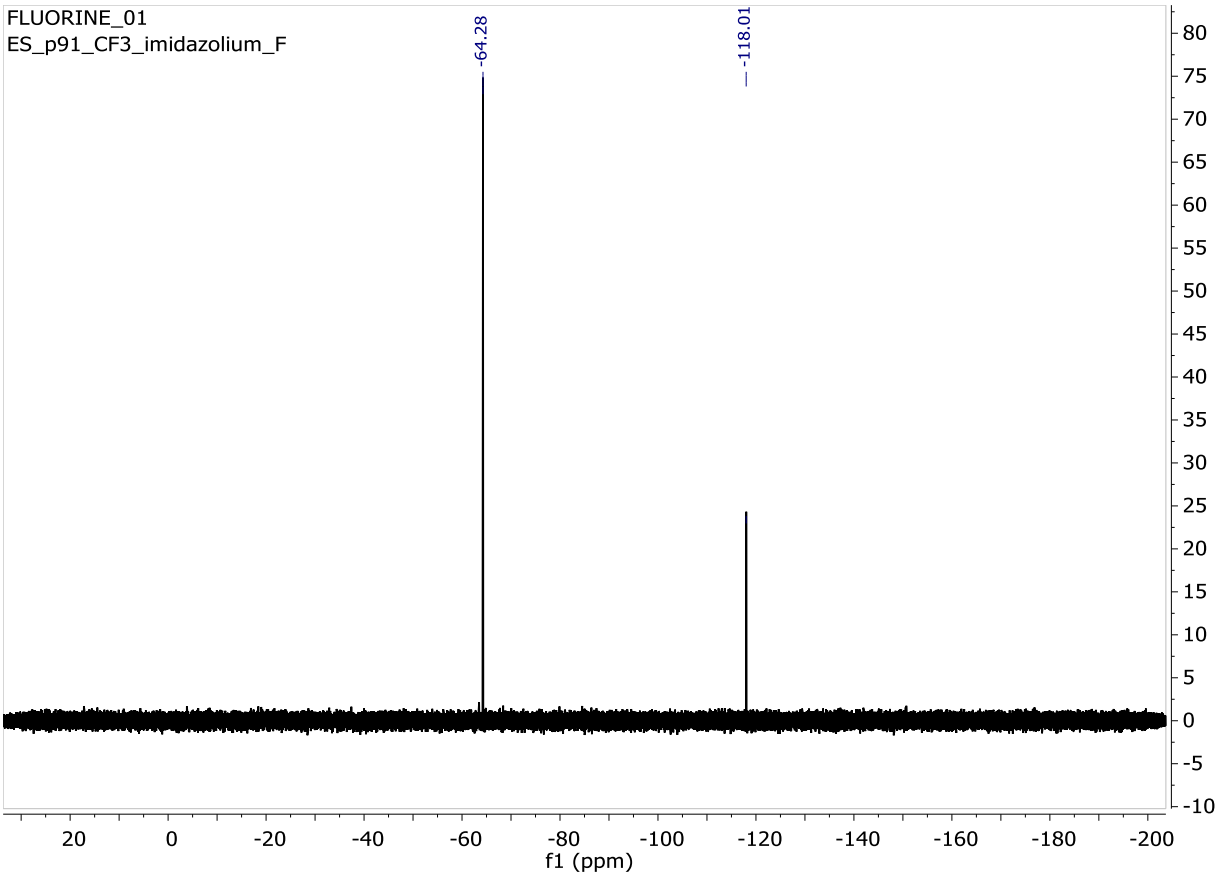

Supplementary Figure 4. ^{19}F NMR CF_3-imidazolium in CD_3CN

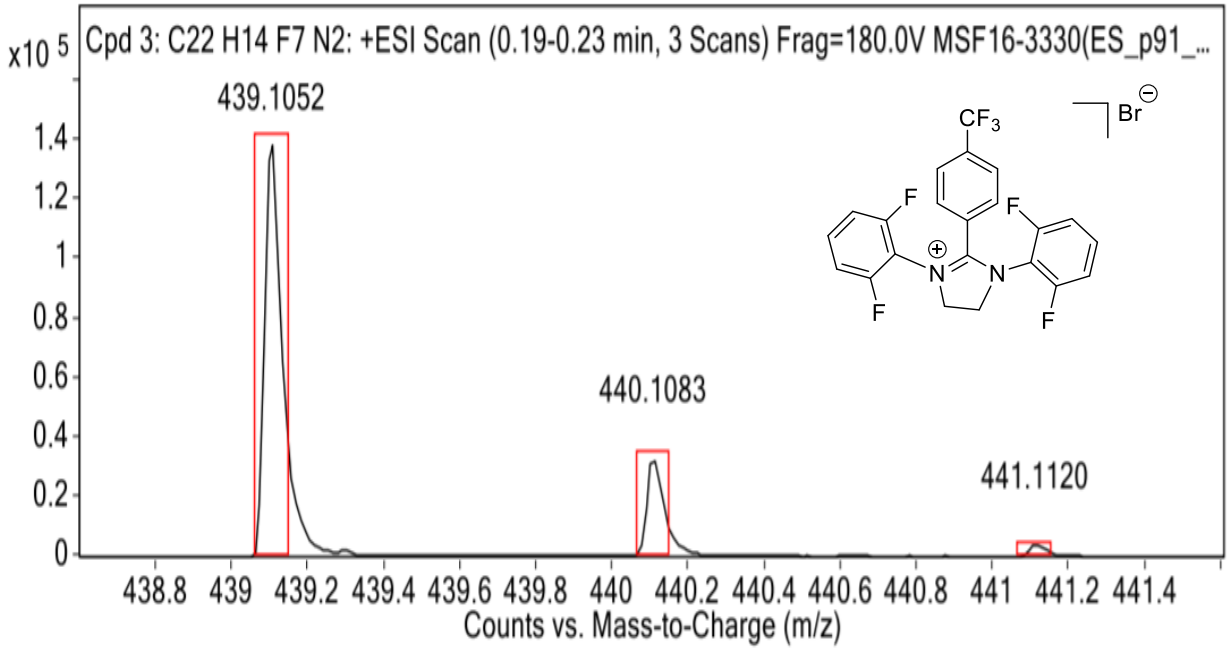

Supplementary Figure 5. ESI Mass Spectrometry CF_3-imidazolium: Observed Mass 439.10520, Calculated Mass: 439.10400

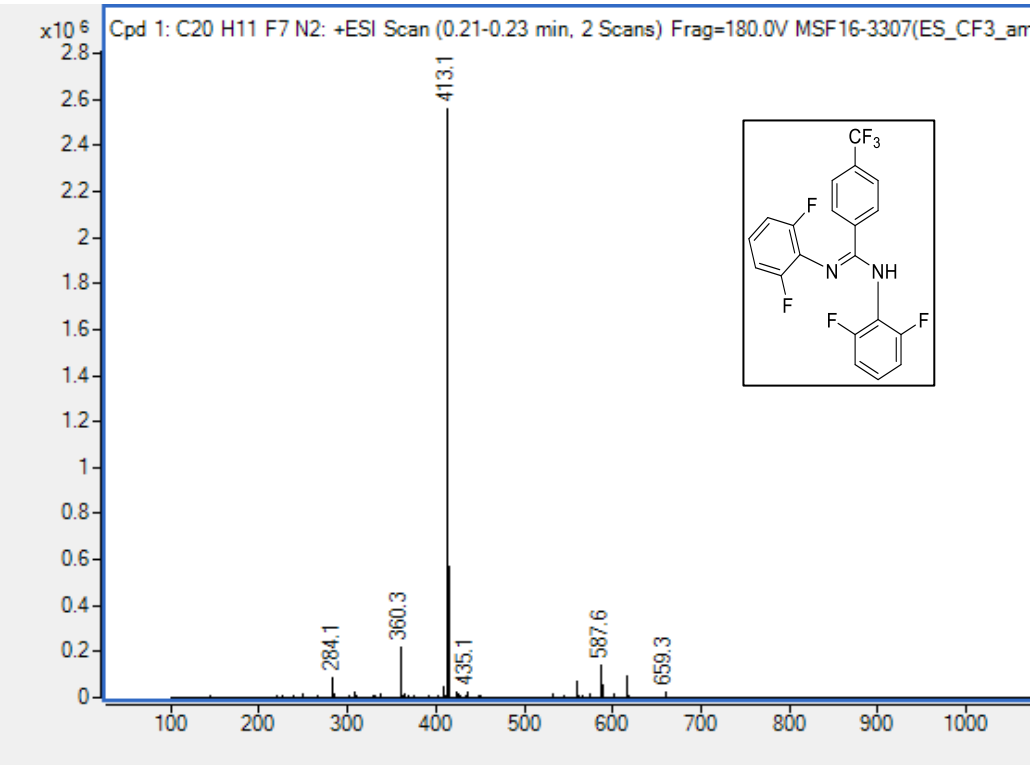

Supplementary Figure 6. ESI Mass Spectrometry CF_3-amidine: Observed Mass 413.08980, Calculated Mass: 413.08830

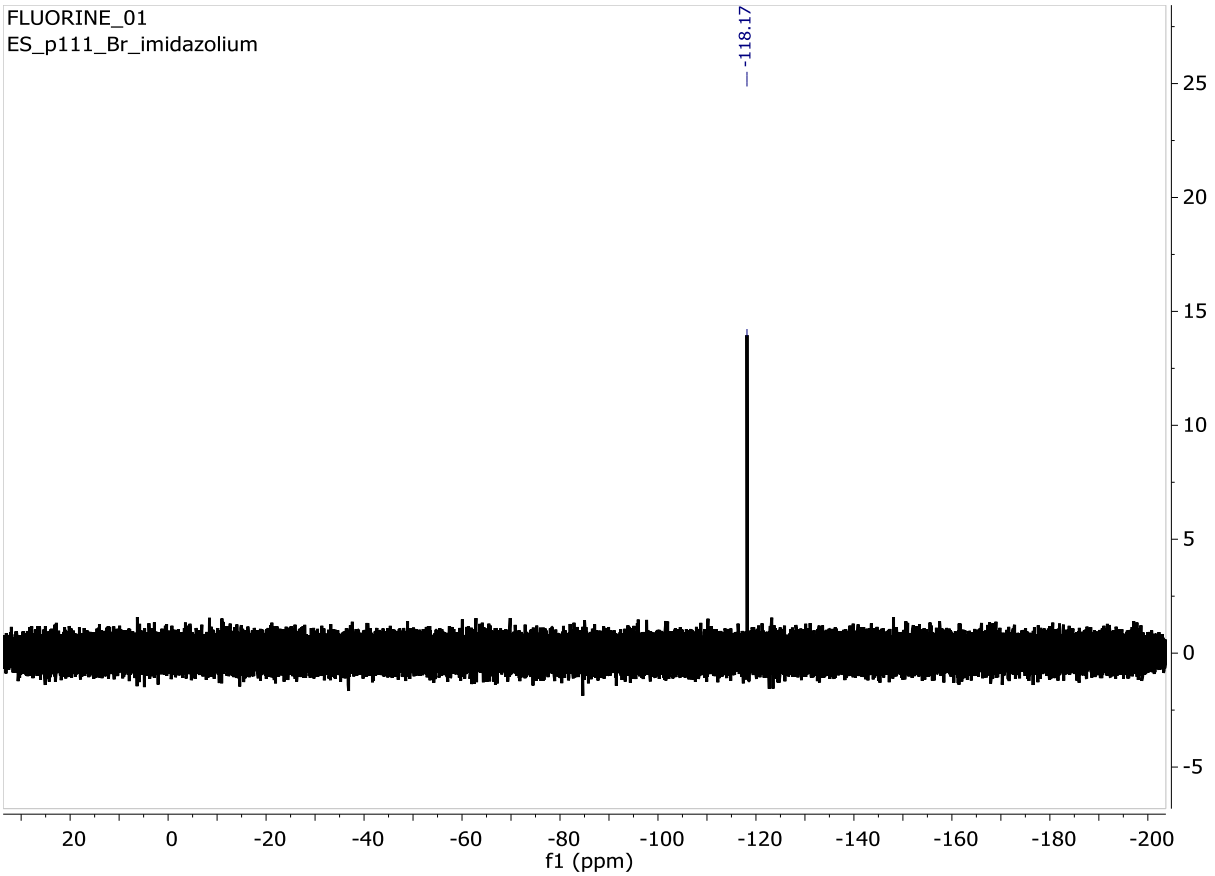

Supplementary Figure 7. ^{19}F NMR Br-imidazolium in CD_3CN

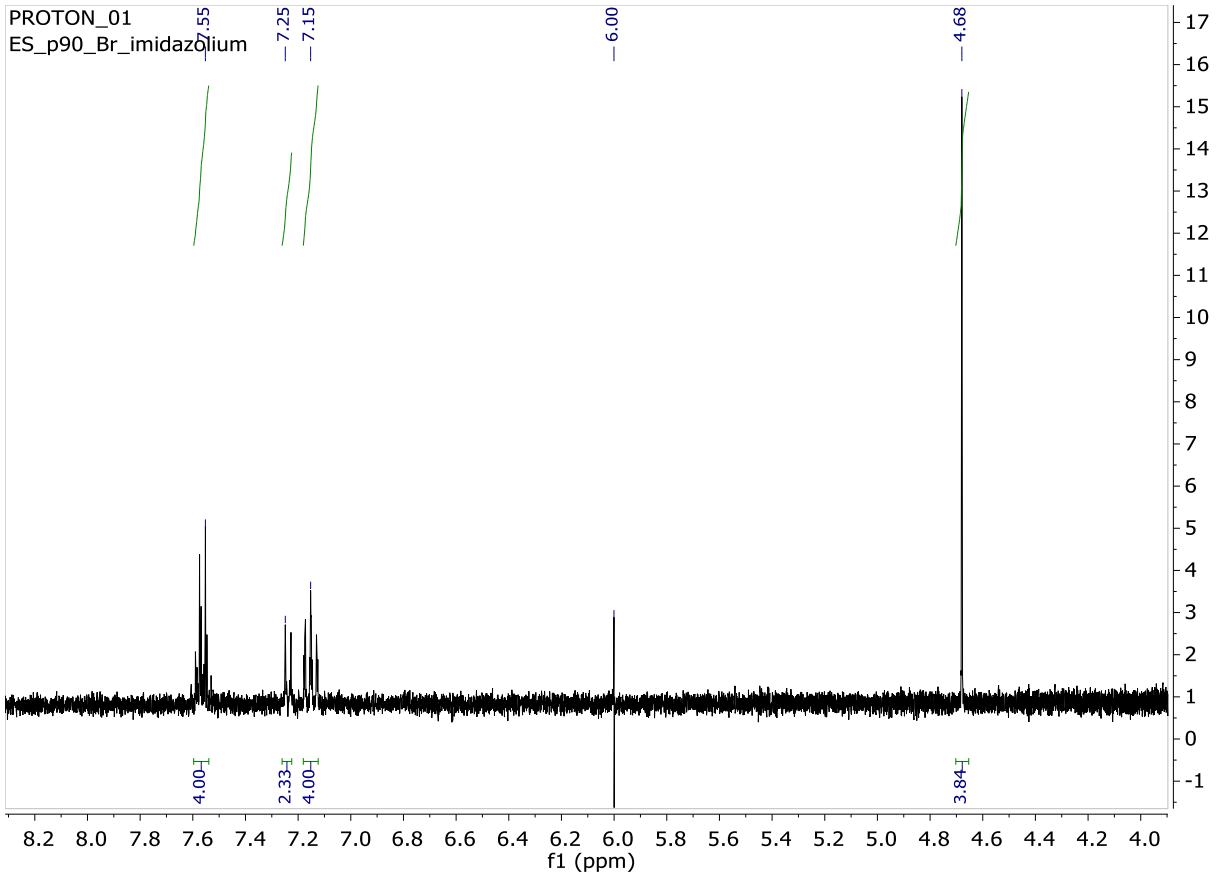

Supplementary Figure 8. ^{1}H NMR Br-imidazolium in CD_3CN

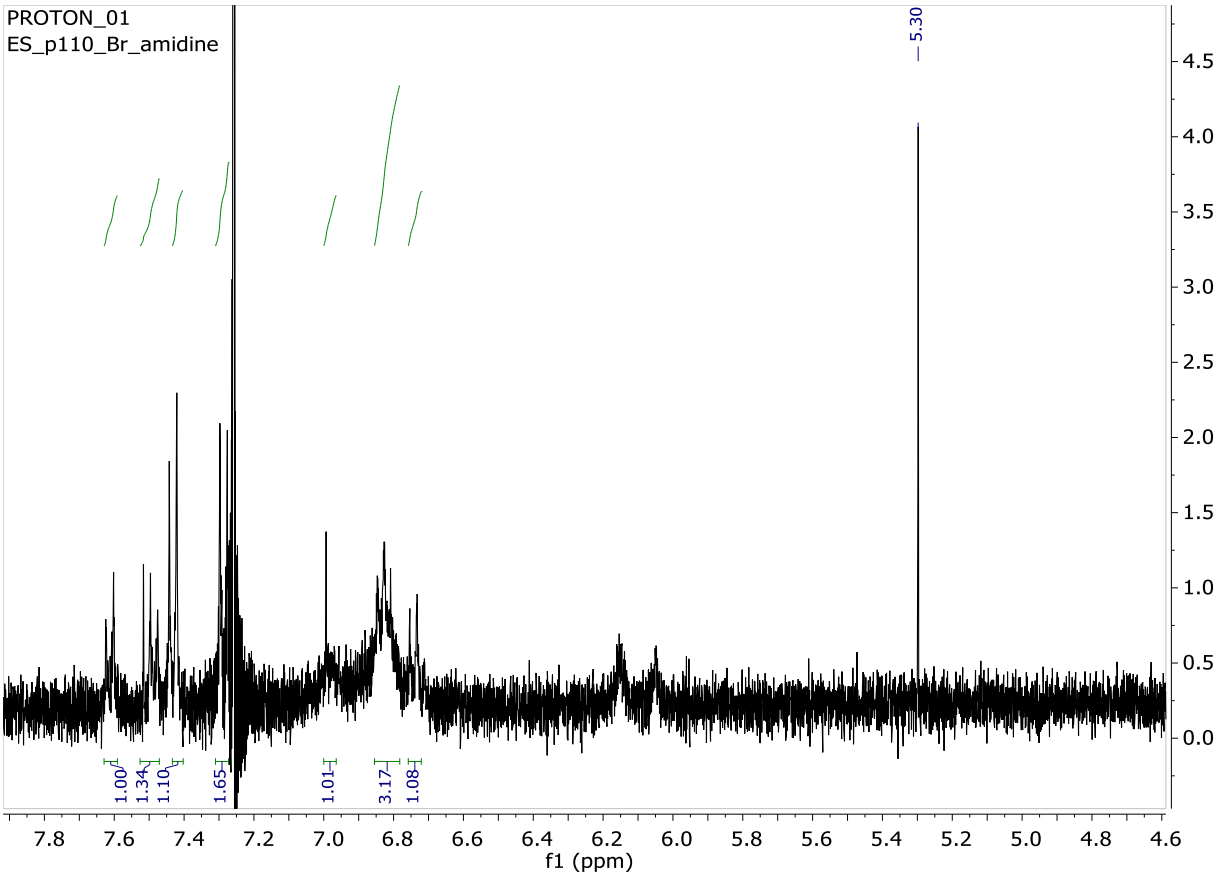

Supplementary Figure 9. ^{1}H NMR Br-amidine in $CDCl_3$

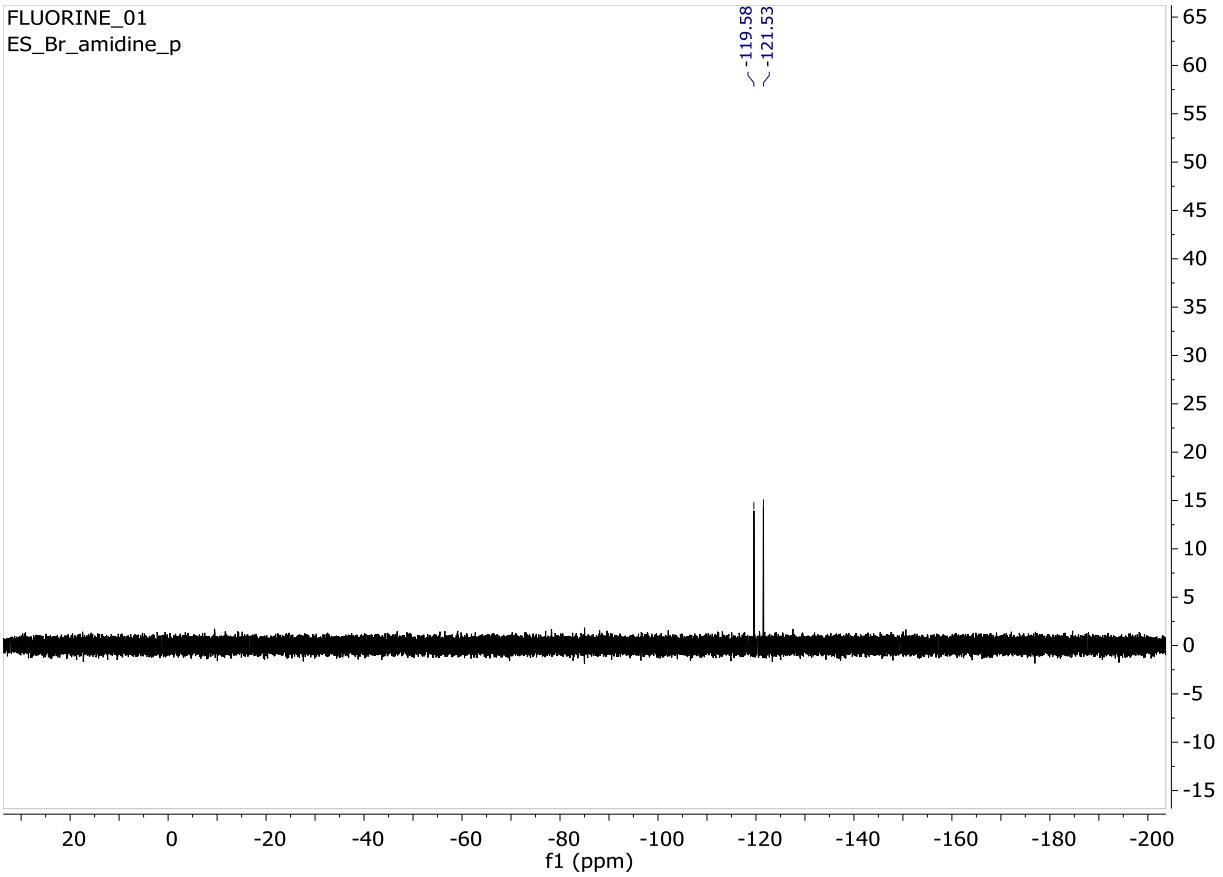

Supplementary Figure 10. ^{19}F NMR CF_3-imidazolium in $CDCl_3$

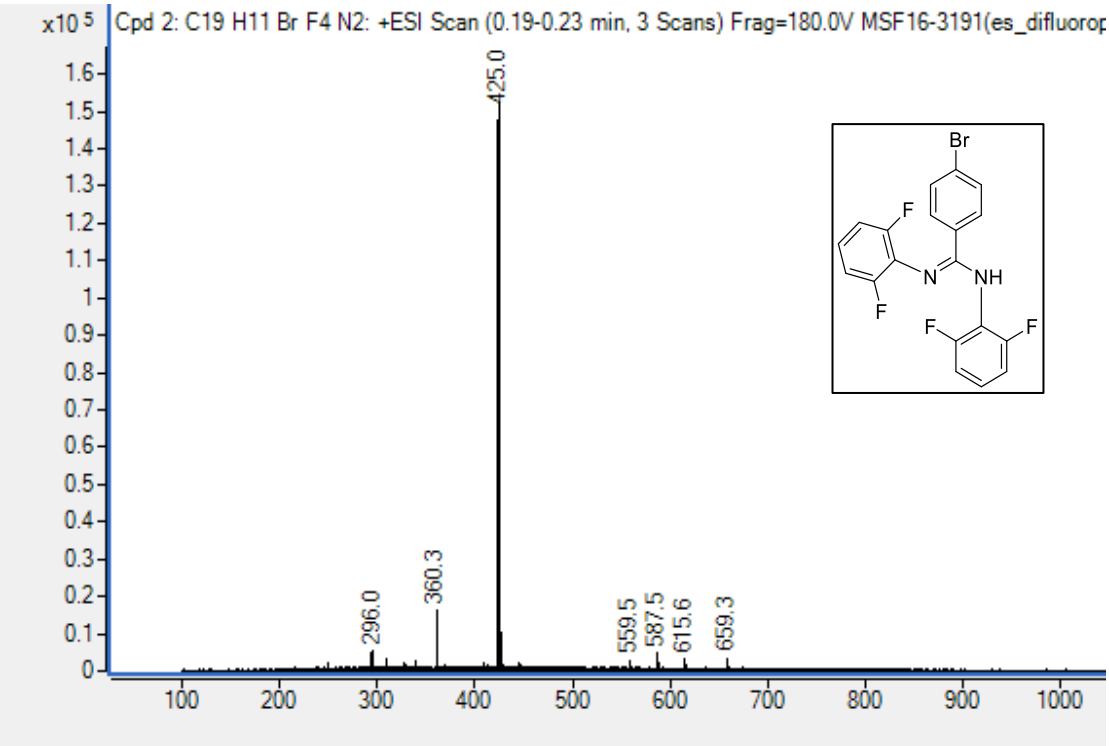

Supplementary Figure 11. ESI Mass Spectrometry Br-amidine: Observed Mass 423.01170, Calculated Mass: 423.01150

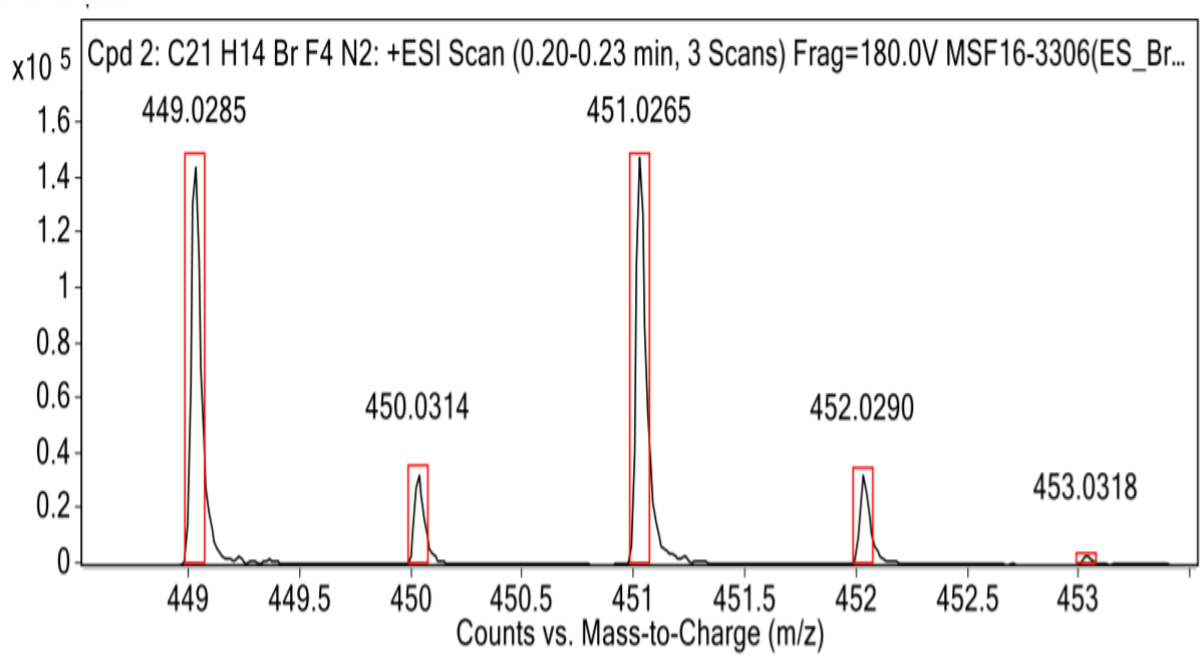

Supplementary Figure 12. ESI Mass Spectrometry Br-amidine: Observed Mass 449.0285, Calculated Mass: 449.02710

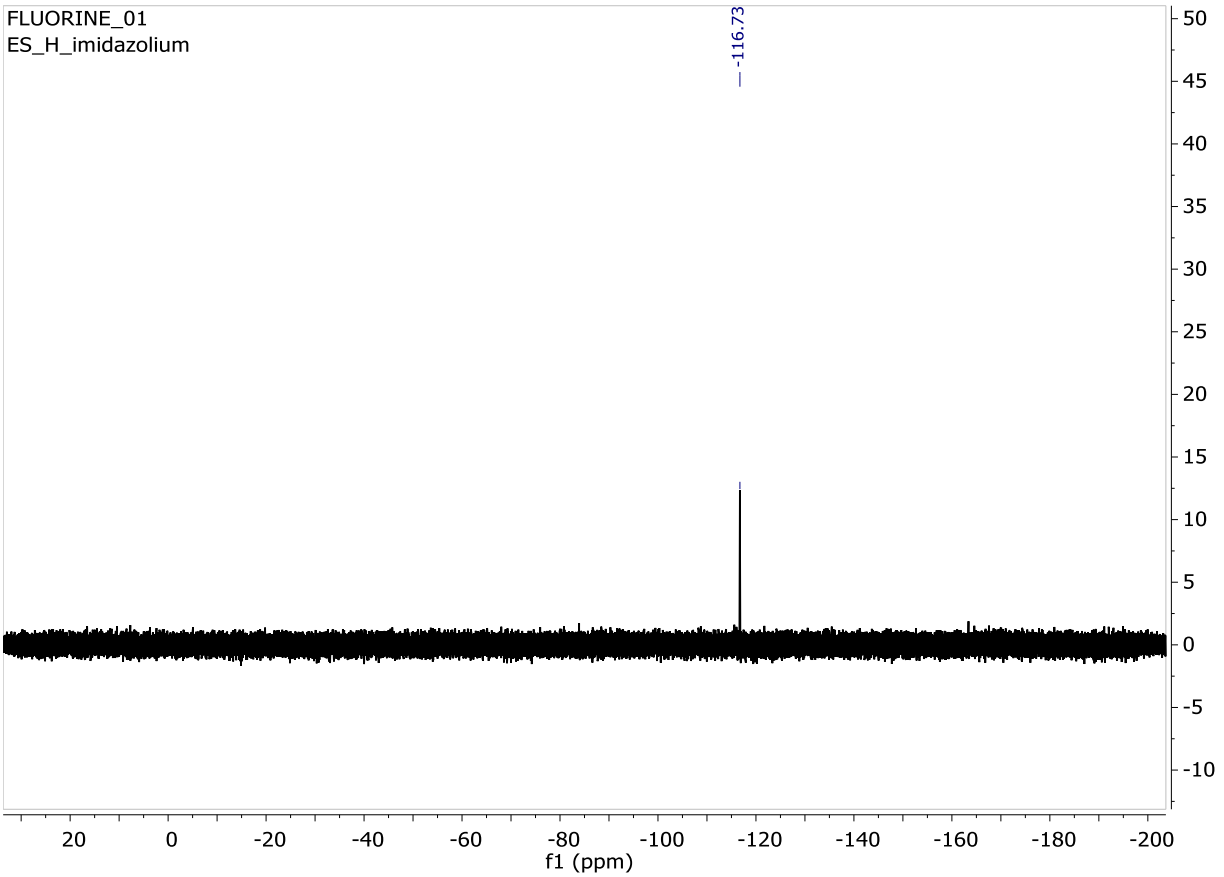

Supplementary Figure 13. ^{19}F NMR H-imidazolium in $CDCl_3$

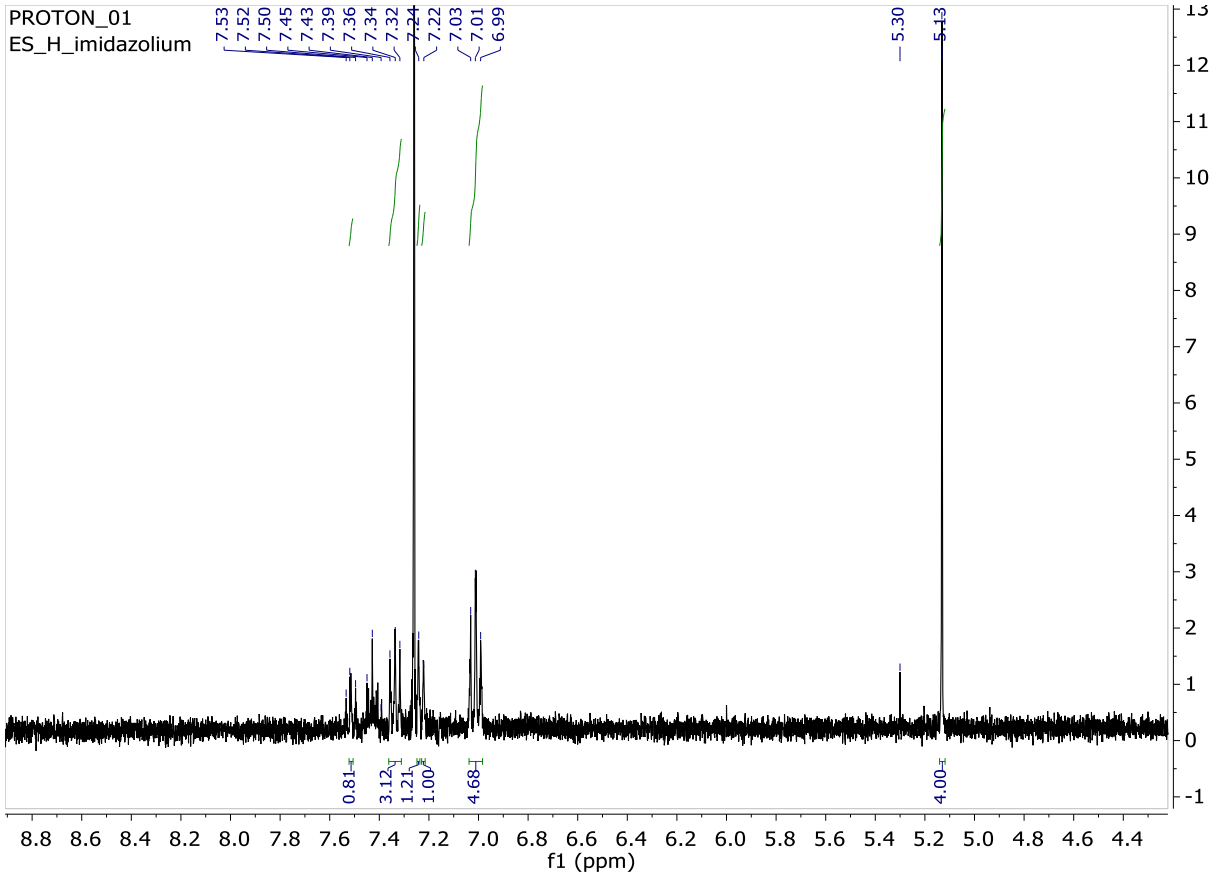

Supplementary Figure 14. ^{1}H NMR H-imidazolium in $CDCl_3$

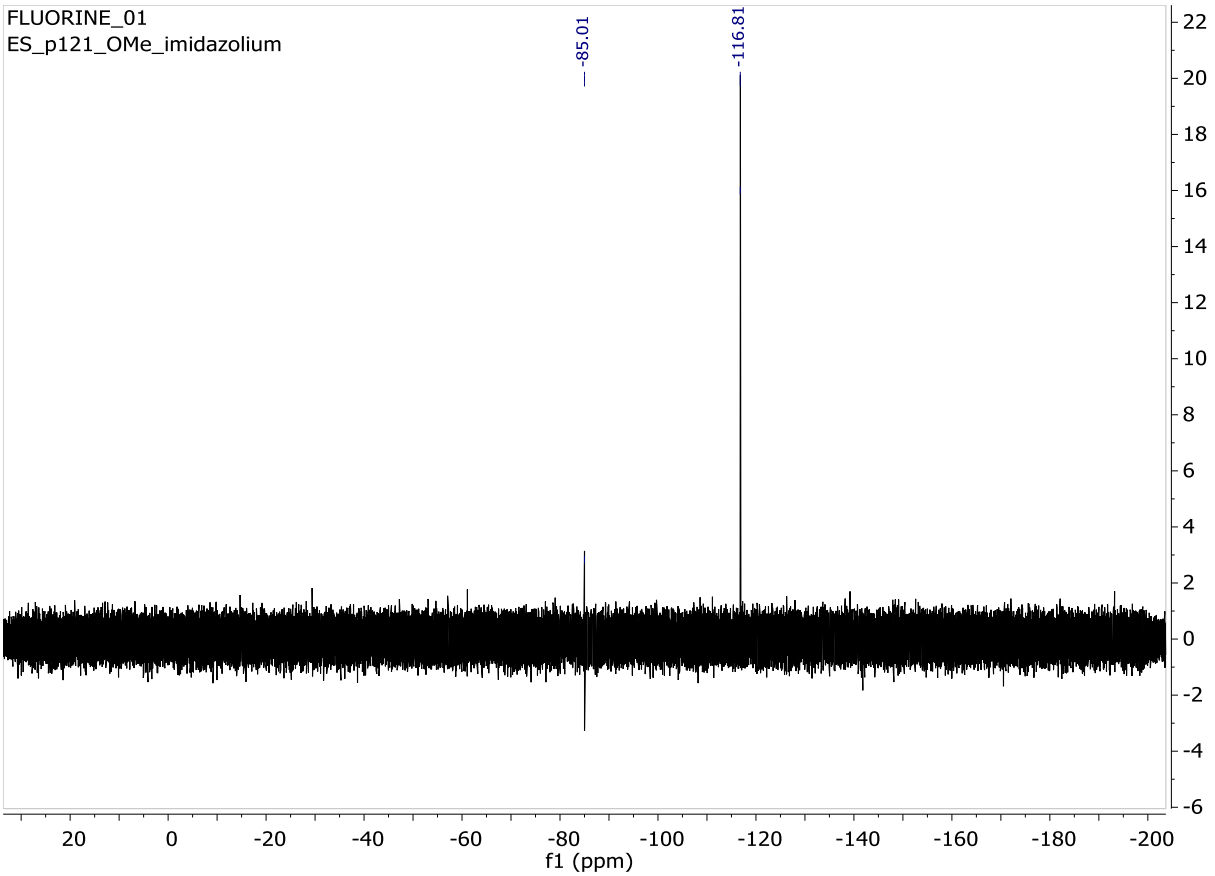

Supplementary Figure 15. ^{19}F NMR H-imidazolium in $CDCl_3$

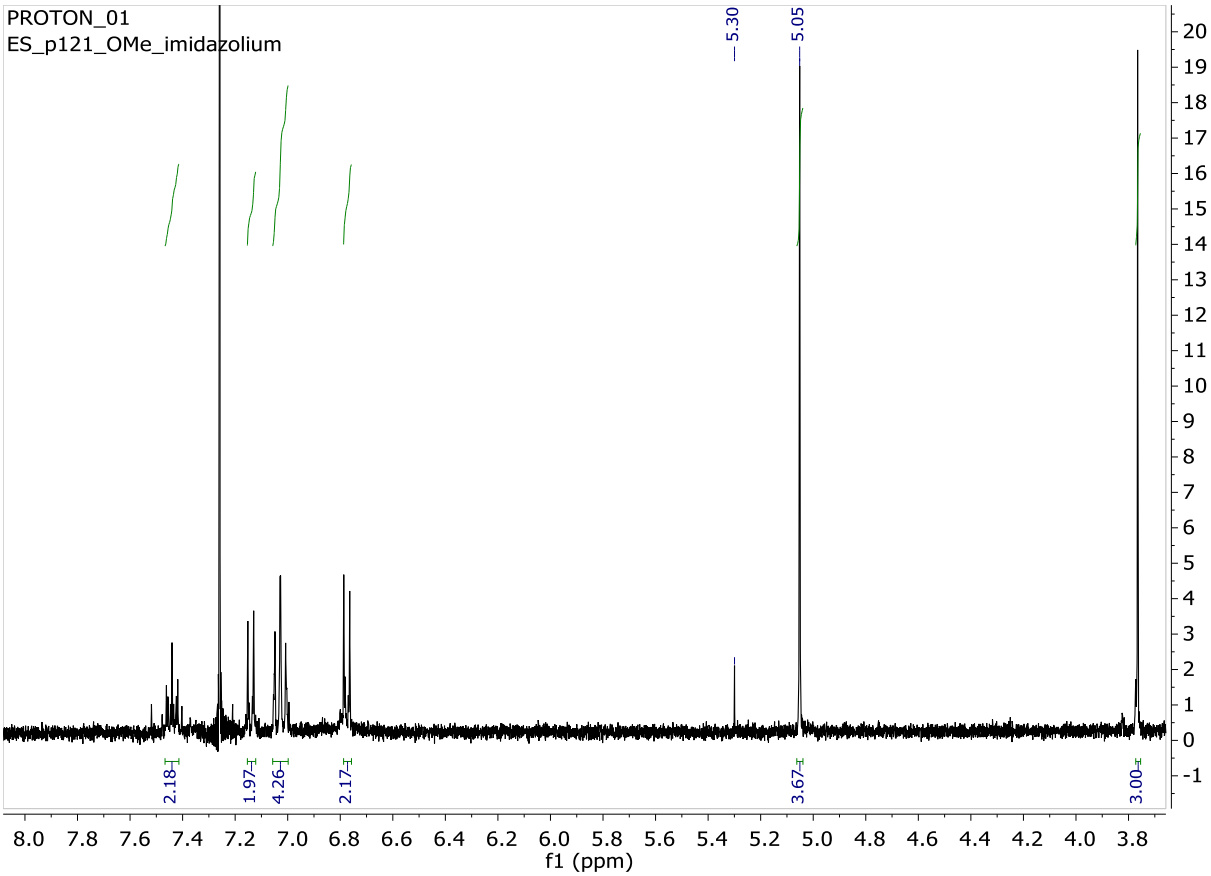

Supplementary Figure 16. ^{1}H NMR OMe-imidazolium in $CDCl_3$

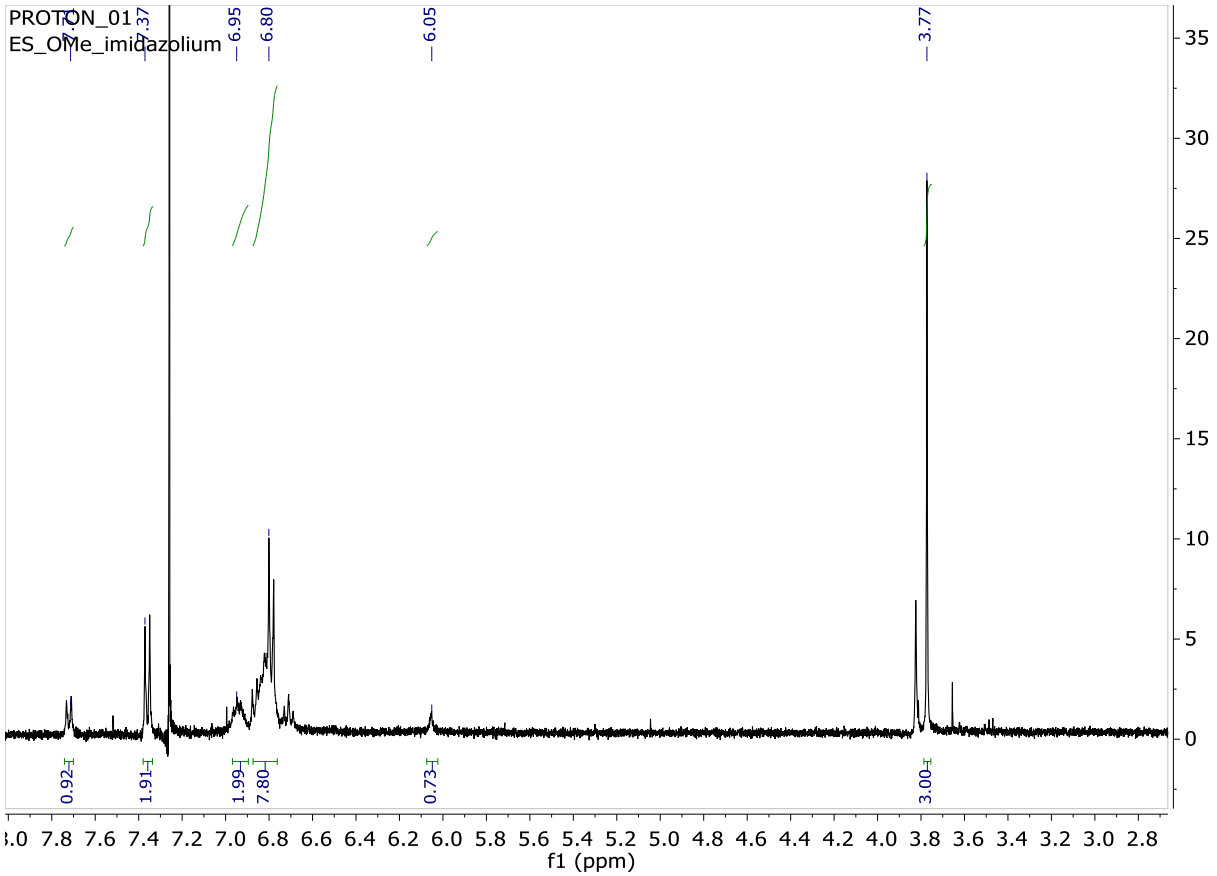

Supplementary Figure 17. ^{1}H NMR OMe-amidine in $CDCl_3$

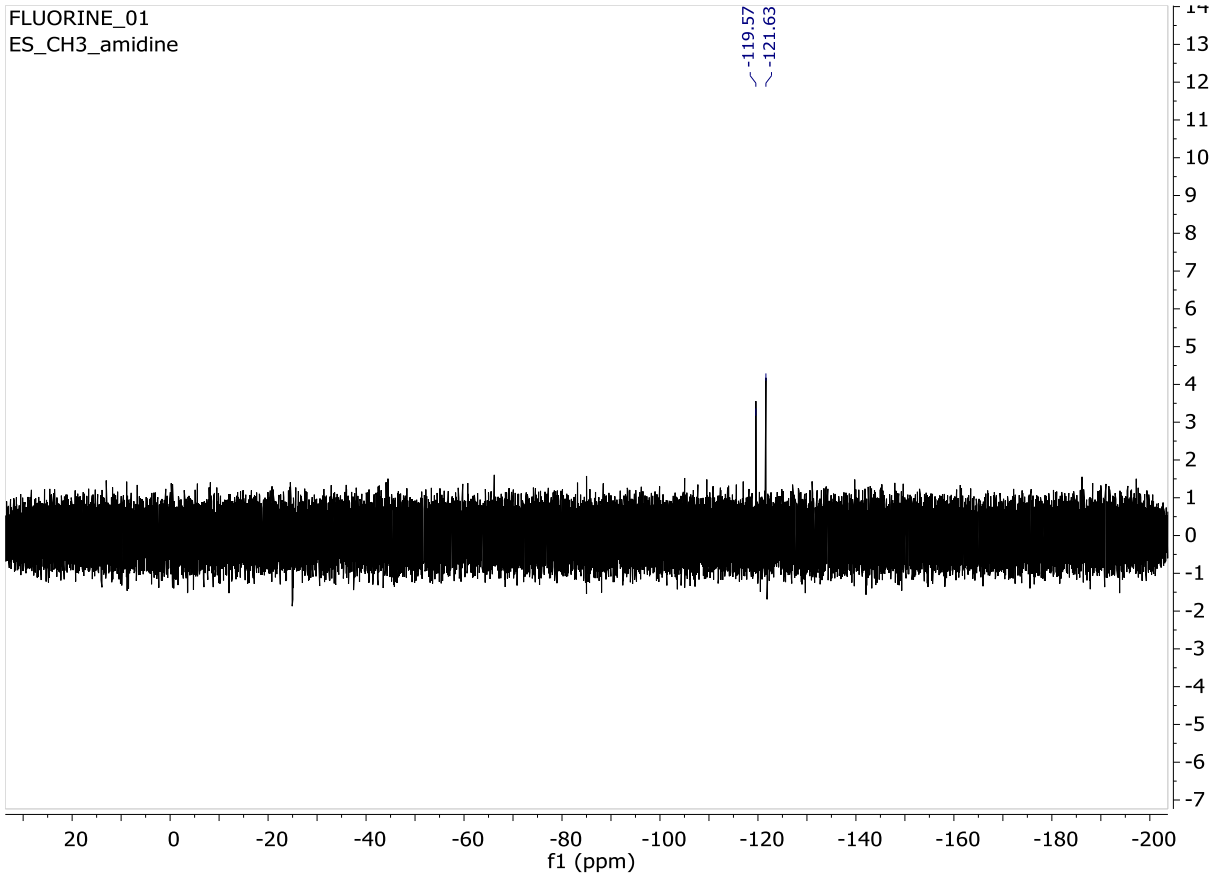

Supplementary Figure 18. ^{19}F NMR CH_3-amidine in $CDCl_3$

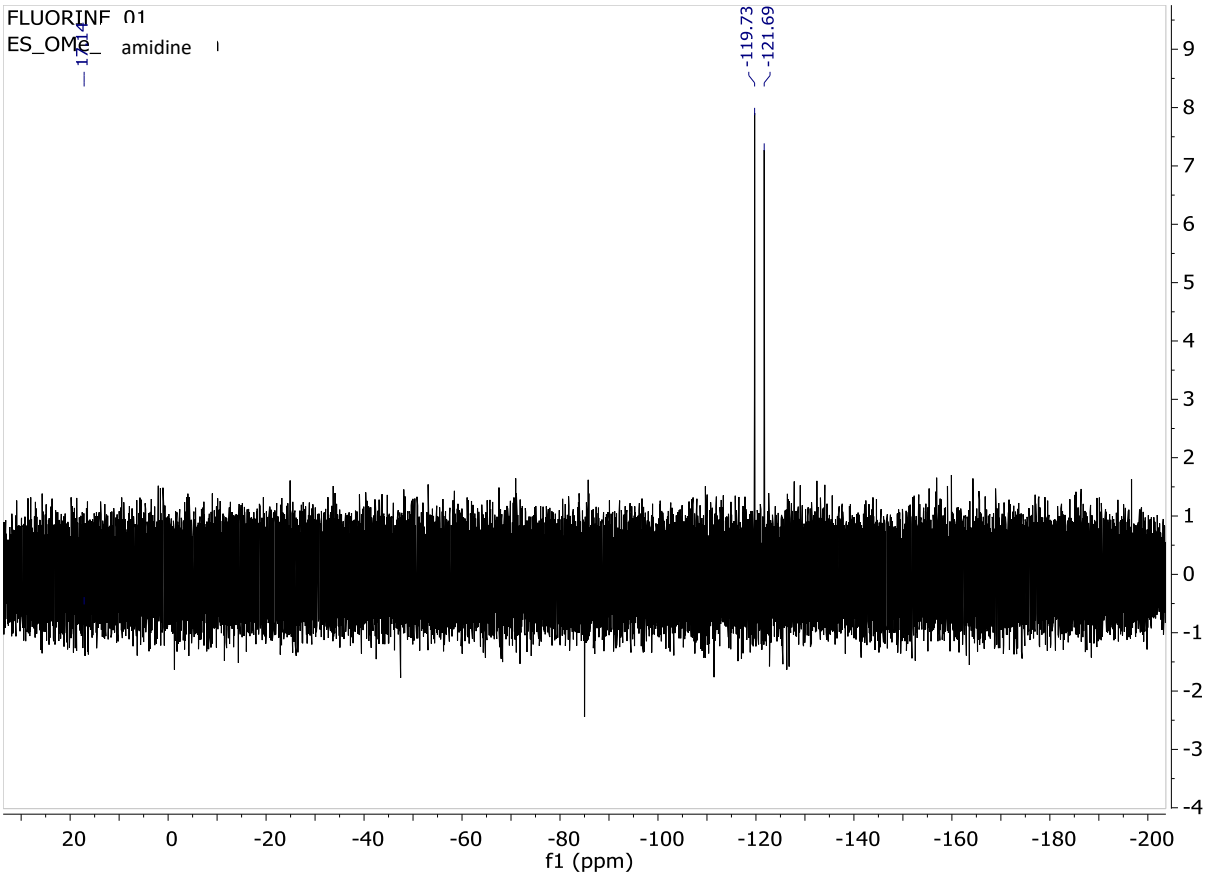

Supplementary Figure 19. ^{19}F NMR OMe-amidine in $CDCl_3$

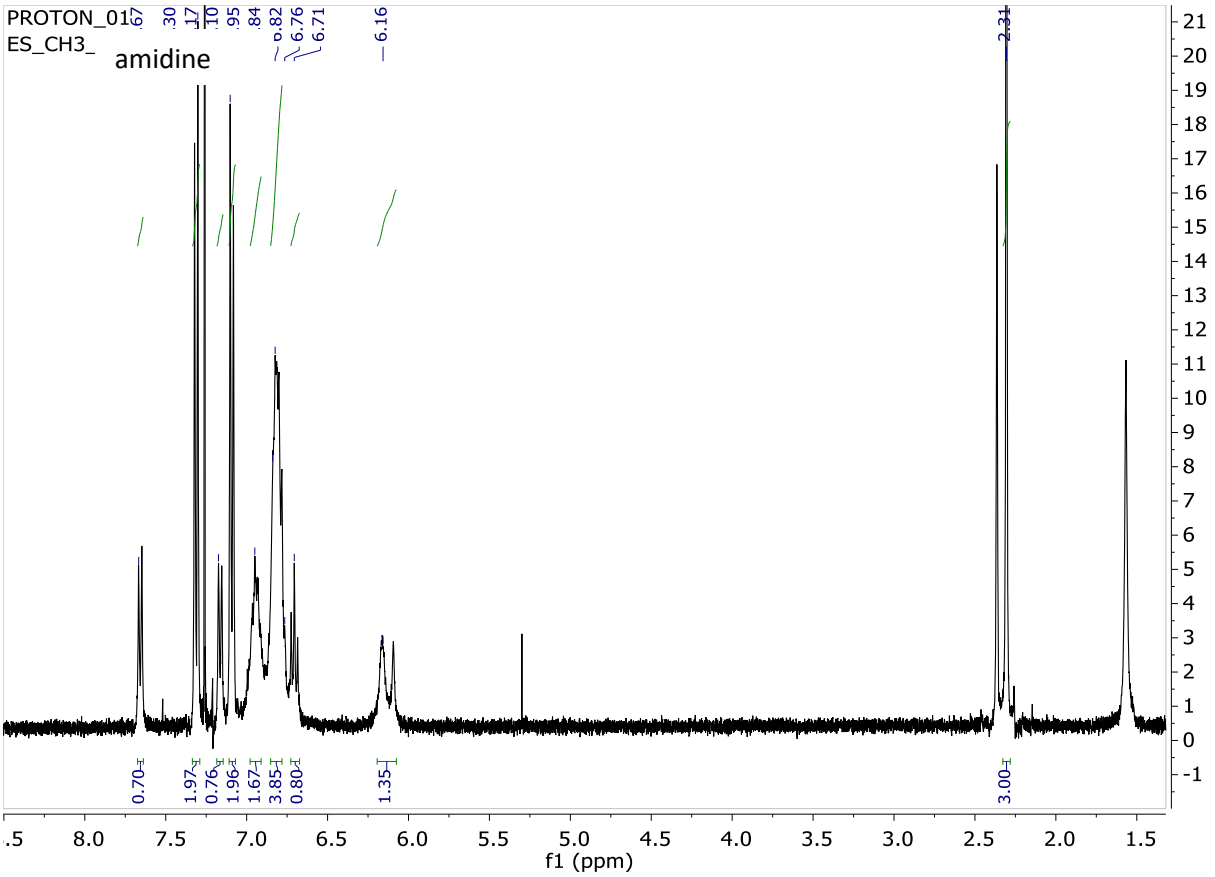

Supplementary Figure 20. ^{1}H NMR CH_3-amidine in $CDCl_3$

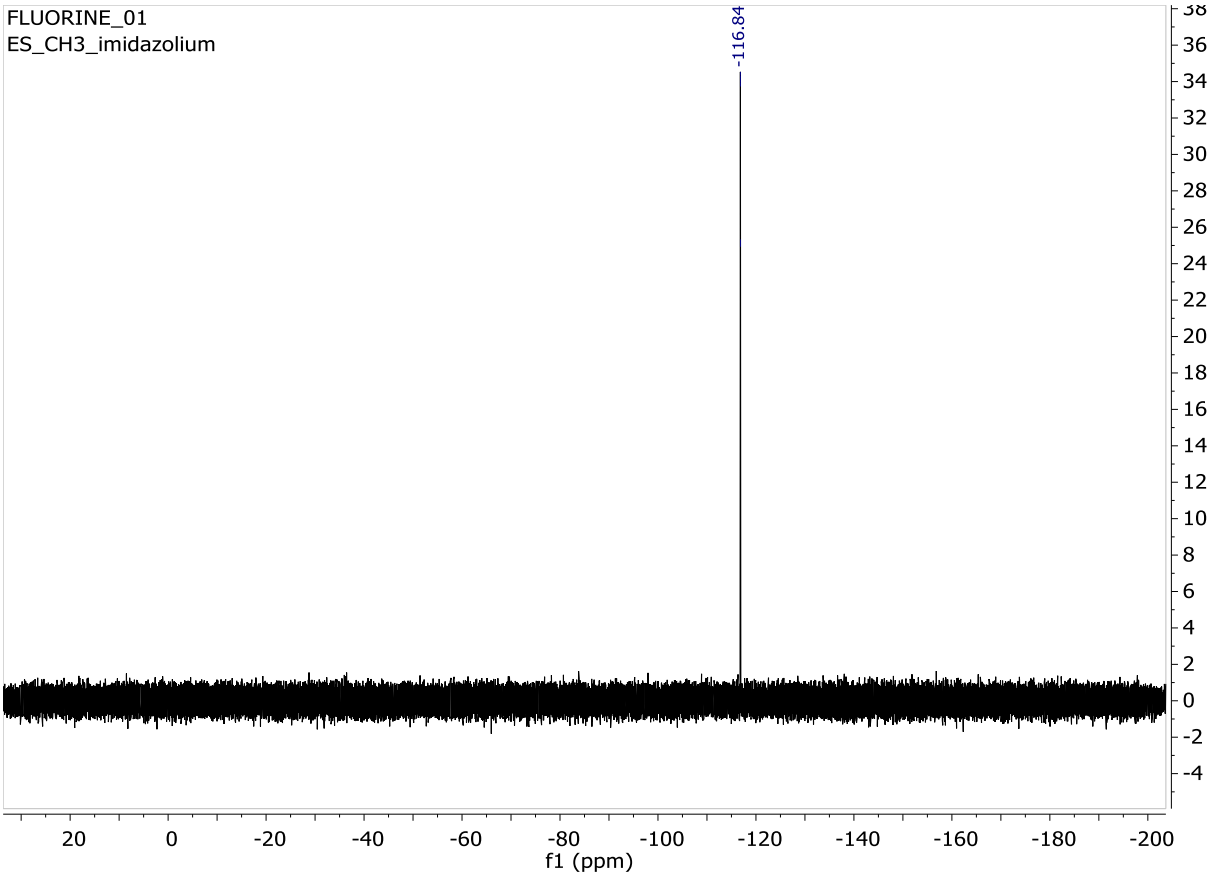

Supplementary Figure 21. ^{19}F NMR CH_3-imidazolium in $CDCl_3$

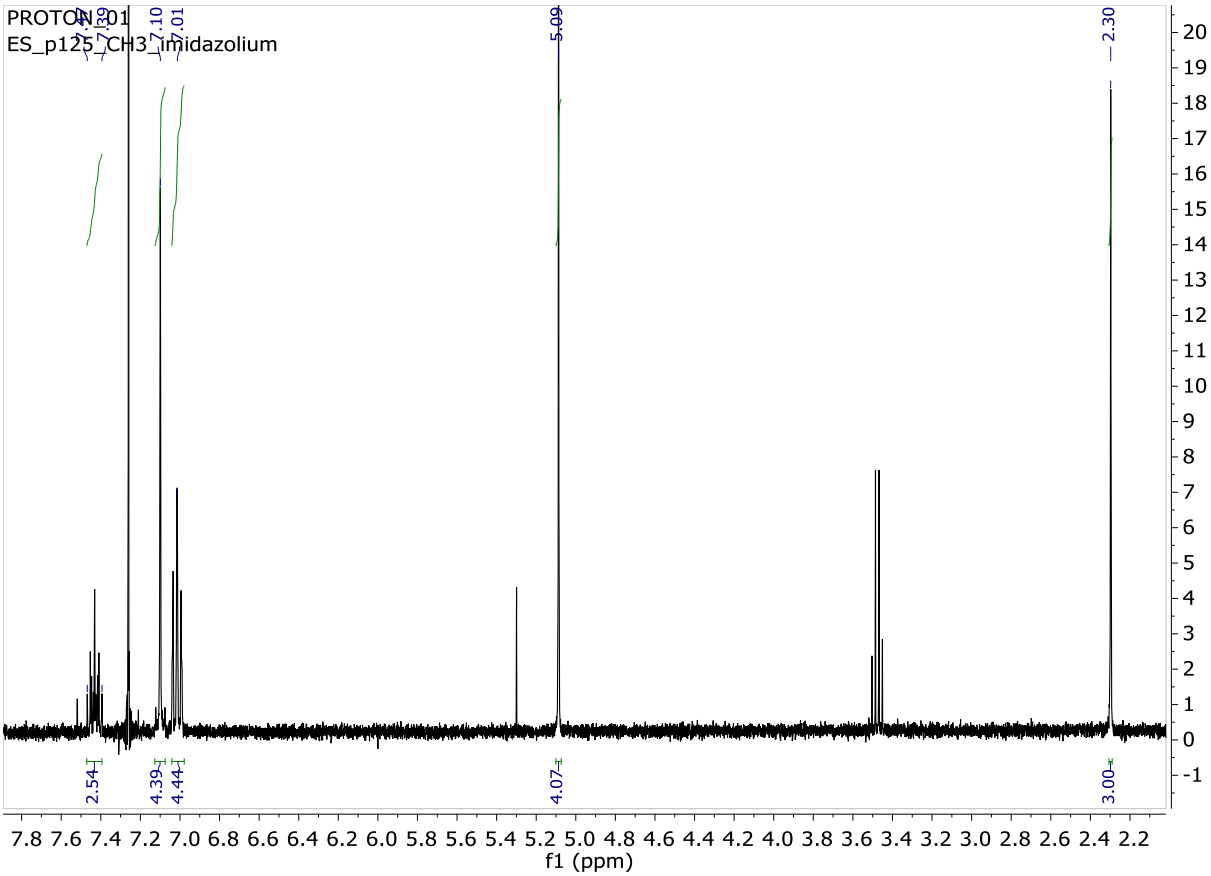

Supplementary Figure 22. ^{1}H NMR CH_3-imidazolium in $CDCl_3$

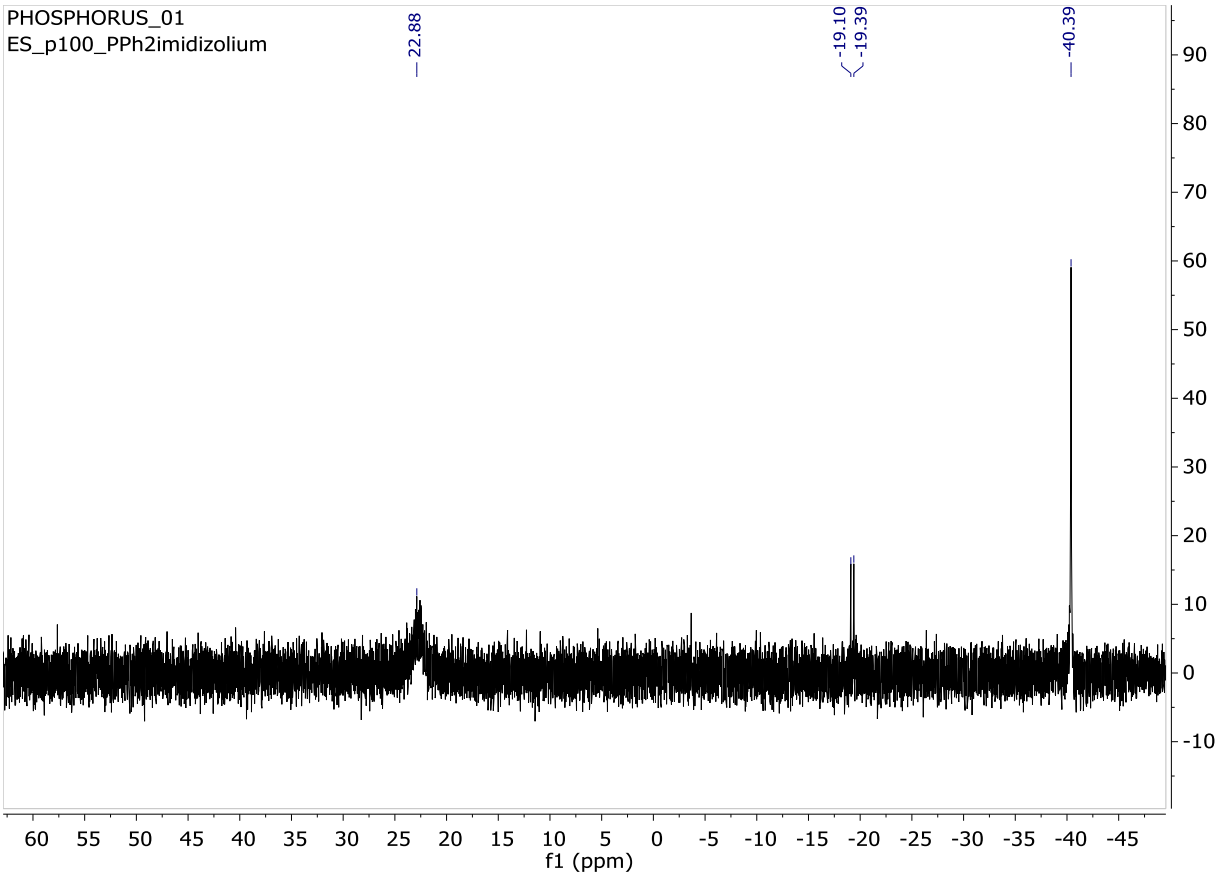

Supplementary Figure 23. ^{31}P NMR PPh_2-imidazolium in $CDCl_3$

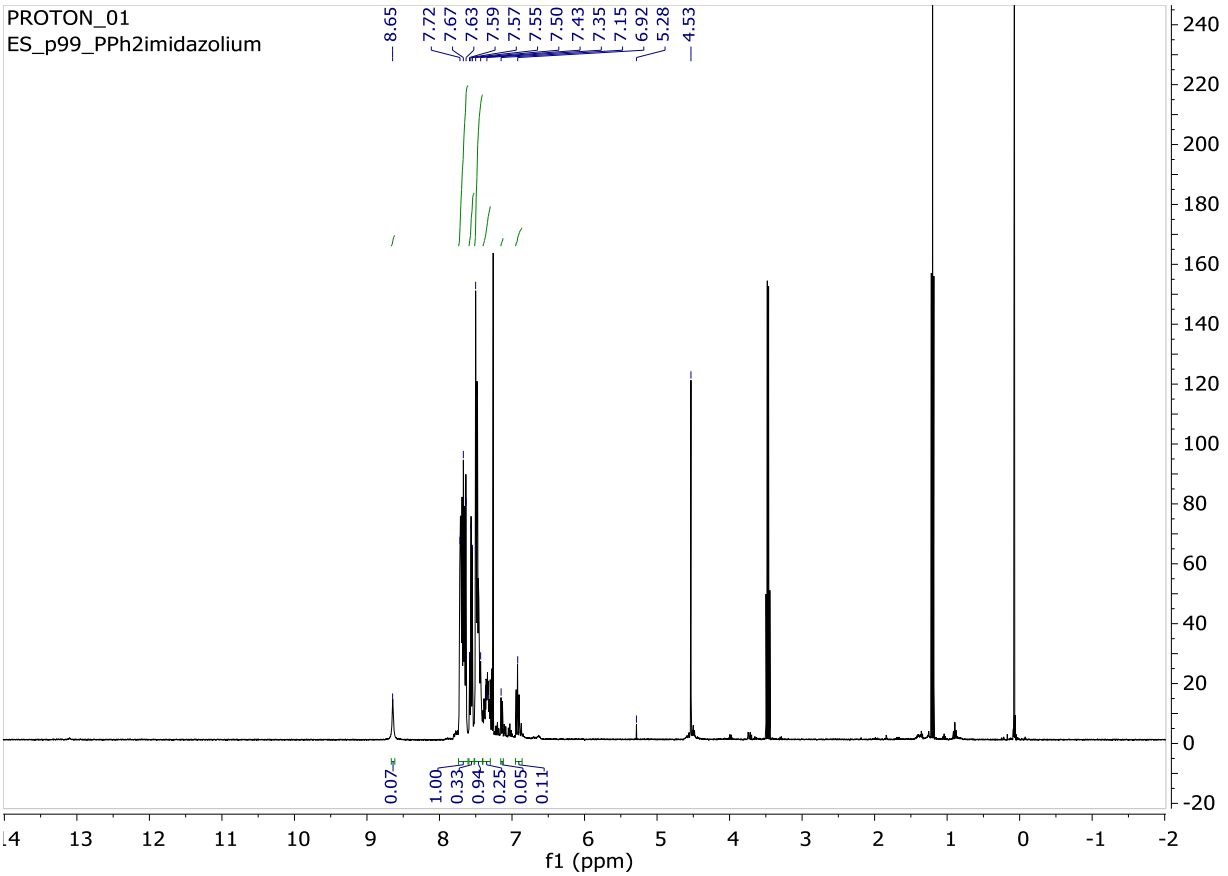

Supplementary Figure 24. ^{1}H NMR PPh_2-imidazolium in $CDCl_3$

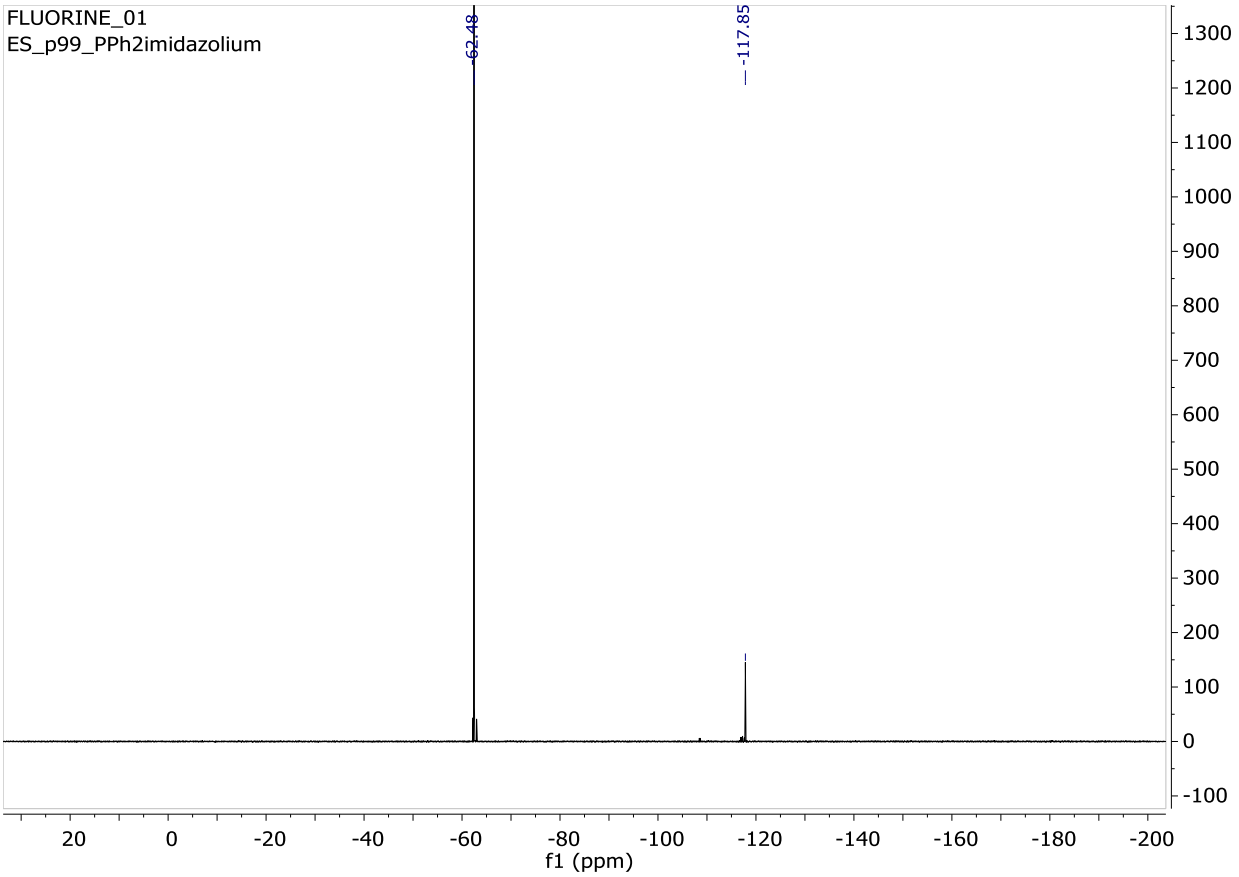

Supplementary Figure 25. ^{19}F NMR PPh_2-imidazolium in $CDCl_3$